Multiscale fluctuations near a Kondo breakdown quantum critical point

I. Paul,[1,2] C. Pépin,[3] and M. R. Norman[2]
[1]*Institut Laue-Langevin, 6 rue Jules Horowitz, BP 156, 38042 Grenoble, France*
[2]*Materials Science Division, Argonne National Laboratory, Argonne, Illinois 60439, USA*
[3]*SPhT, CEA-Saclay, L'Orme des Merisiers, 91191 Gif-sur-Yvette, France*
(Received 10 April 2008; revised manuscript received 10 June 2008; published 9 July 2008)

We study the Kondo-Heisenberg model using a fermionic representation for the localized spins. The mean-field phase diagram exhibits a zero-temperature quantum critical point separating a spin liquid phase where the f-conduction hybridization vanishes and a Kondo phase where it does not. Two solutions can be stabilized in the Kondo phase, namely, a uniform hybridization when the band masses of the conduction electrons and the f spinons have the same sign and a modulated one when they have opposite sign. For the uniform case, we show that above a very small Fermi-liquid temperature scale, the critical fluctuations associated with the vanishing hybridization have dynamical exponent $z=3$, giving rise to a specific-heat coefficient that diverges logarithmically in temperature, as well as a conduction-electron inverse lifetime that has a $T \log T$ behavior. Because the f spinons do not carry current, but act as an effective bath for the relaxation of the current carried by the conduction electrons, the latter result also gives rise to a $T \log T$ behavior in the resistivity. This behavior is consistent with observations in a number of heavy fermion metals.

DOI: 10.1103/PhysRevB.78.035109 PACS number(s): 71.27.+a, 72.15.Qm, 75.20.Hr, 75.30.Mb

I. INTRODUCTION

A large number of experiments have been performed on metallic heavy fermion compounds close to a zero-temperature phase transition [a quantum critical point (QCP)] driven by applied magnetic field, chemical doping, or pressure.[1,2] In the quantum critical regime, the thermodynamics and transport properties indicate a breakdown of the Fermi liquid. In many cases, the resistivity is quasilinear in temperature over several decades, and the specific-heat coefficient diverges logarithmically. The spin susceptibility typically exhibits an anomalous exponent in temperature. Neutron scattering experiments on some of these materials have revealed that the anomalous exponent in the dynamical susceptibility is identical for all points in the Brillouin zone,[3,4] suggesting a local character for the fluctuations. de Haas–van Alphen (dHvA) experiments also find a divergence of the effective mass when approaching the critical point, along with a change in the Fermi-surface topology when going through it.[5]

These unusual observations have motivated many theoretical studies that have attempted to capture these effects. Most theories[2,6–9] are based on the assumption that at the QCP, a spin-density wave forms, and therefore the critical fluctuations that destabilize the Fermi liquid are magnetic in nature.[2,6–9] In three dimensions, these theories fail to capture simultaneously the linear temperature dependence of the resistivity, the logarithmic divergence of the specific-heat coefficient,[10] and the anomalous exponent of the spin susceptibility.[11] For an antiferromagnetic spin-density wave transition, a central problem is that the critical fluctuations are confined to an inverse coherence length about the spin-density ordering vector, and consequently, only parts of the Fermi surface couple effectively with the critical bosonic modes.

More recently, the problem has been approached from another perspective which takes the point of view that at the QCP, magnetic fluctuations suppress the formation of the heavy Fermi liquid, driving the effective Kondo temperature of the lattice (T_K) to zero.[10] This has studied from a variety of approaches, including extended dynamical mean-field theory,[12] cluster dynamical mean-field theory,[13,14] and a slave boson approach.[15,16] In this picture, the QCP is a fractionalized critical point at which the heavy quasiparticle deconfines into a spinon and holon. One feature that distinguishes between these two classes of theories is that the first predicts the Fermi surface to change smoothly across the QCP, while the second predicts an abrupt change.[10] Recent results of the Hall effect for $YbRh_2Si_2$,[17] as well as the earlier mentioned dHvA data,[5] have lent support to theories of the second type.

Here, we explore the possibility that in the quantum critical regime, the magnetic fluctuations are not the dominant ones at the QCP and that the unusual behavior in thermodynamics and transport is due to critical fluctuations of a nonmagnetic order parameter associated with the vanishing energy scale T_K. One motivation for this point of view is the fact that in some compounds such as $YbRh_2Si_2$, the gain in entropy inside the magnetically ordered phase represents only a few percent of the total entropy per localized spin.[18] The order parameter we advocate is the field σ associated with the hybridization between the localized spins and the conduction electrons.[19,20] At the QCP, the effective Kondo temperature for the lattice goes to zero, leading to a "Kondo breakdown" of the heavy Fermi liquid. The critical fluctuations of σ are gapless excitations, and we study how these fluctuations influence the properties of the metal using the formalism of the large N Kondo-Heisenberg model.

There have been several earlier studies of this model.[15,16,21] Beyond the mean-field level, the Kondo-Heisenberg model can be treated as a lattice gauge theory. Senthil *et al.*[15] examined the effect of the gauge fluctuations in this model, while Coleman *et al.*[16] studied the zero-temperature transport anomalies. Although our work closely follows that of Ref. 15, we find a number of effects associ-

ated with the fluctuations of the σ field which were not discovered in these earlier studies.

At the Kondo breakdown QCP, the metal passes from a magnetic phase (which we approximate, as in earlier work,[15] as a uniform spin liquid) to a Kondo phase. In the spin liquid phase, the f spinons are characterized by a "Fermi surface" which generically differs in size from the conduction-electron Fermi surface. In the Kondo phase, these two surfaces become coupled due to the nonzero expectation value of σ. In our study, we observe two phenomena associated with this. First, for the case where the spinon and conduction-electron masses have opposite sign, σ can order at a finite wave vector, leading to spatial modulations of the Kondo hybridization analogous to the Larkin-Ovchinnikov-Fulde-Ferrell (LOFF) state of superconductivity.[22,23] Second, we find the presence of multiple energy scales, spread over a very large range in energy, due to the mismatch between the two Fermi surfaces. The lowest scale, below which Fermi-liquid behavior is restored, is extremely small, above which, up to an ultraviolet cutoff of order the single-ion Kondo temperature, the critical fluctuations of σ exhibit a dynamical exponent $z=3$. This gives rise to a marginal Fermi-liquid-like behavior in $d=3$ for the conduction electrons along the entire Fermi surface, due to scattering with the critical fluctuations. This property is to be contrasted with antiferromagnetic spin-density wave models, where only on parts of the Fermi surface the scattering of the electrons with the critical mode is effective. Next, since the f spinons do not carry current, but act as an effective bath for the relaxation of the current carried by the conduction electrons, the marginal Fermi-liquid behavior also gives rise to a resistivity that goes as $T \log T$. This behavior is unlike either that of ferromagnetic spin-density wave models in which the transport lifetime is less singular than the single-particle lifetime (i.e., in the latter models, forward scattering does not degrade the current) or that of antiferromagnetic spin-density wave models in which the "cold" parts of the Fermi surface dominate the transport properties.[24] Moreover, a logarithmic dependence is found for the specific-heat coefficient from both the gauge[15] and σ fluctuations. The latter also give rise to an anomalous temperature exponent of 4/3 in the uniform spin susceptibility. A summary of our results has been presented in a shorter paper.[25]

The phenomenon of the breakdown of the Kondo effect at a QCP can also be studied in the more general context of a periodic Anderson model. This generalization is discussed in other works.[14,26]

II. MODEL AND FORMALISM

The starting point of our theory is the microscopic Kondo-Heisenberg model in three dimensions,[27] which describes a broad band of conduction electrons interacting with a periodic array of localized spins through antiferromagnetic Kondo coupling $J_K>0$. Additionally, the localized spins interact with one another via nearest-neighbor exchange $J_H>0$. The Hamiltonian for the large N version of this model, where N denotes the enlarged spin symmetry group $SU(N)$, is given by

$$\mathcal{H} = -t\sum_{\langle ij\rangle,\alpha} c_{i\alpha}^{\dagger}c_{j\alpha} + \frac{J_K}{N}\sum_{i,\alpha,\beta} c_{i\alpha}^{\dagger}c_{i\beta}f_{i\beta}^{\dagger}f_{i\alpha} + \frac{J_H}{N}\sum_{\langle ij\rangle,\alpha,\beta} f_{i\alpha}^{\dagger}f_{i\beta}f_{j\beta}^{\dagger}f_{j\alpha}. \tag{1}$$

Here $c_{i\alpha}^{\dagger}$ ($c_{i\alpha}$) are creation (annihilation) operators for the conduction electrons with spin index $\alpha=(1,N)$ at site i and $\langle ij\rangle$ refers to nearest-neighbor sites. t is the hopping matrix element between neighboring sites for the conduction electrons. The $SU(N)$ generalization of the localized spins S_i^a, with $a=(1, \ldots, N^2-1)$ at each site i, is expressed in terms of Abrikosov pseudofermions (or spinons) by $S_i^a = \Sigma_{\alpha\beta} f_{i\alpha}^{\dagger}(\Gamma_{\alpha\beta}^a/N) f_{i\beta}$, where Γ^a are the generators of the $SU(N)$ group in the fundamental representation. This fermionic representation of the spin operator gives rise to a local constraint at each site, i,

$$\sum_{\alpha} f_{i\alpha}^{\dagger}f_{i\alpha} = \frac{N}{2}, \quad \forall\, i. \tag{2}$$

We note that in the context of the heavy fermion systems, the Heisenberg exchange term is often equated to the Ruderman-Kittel-Kasuya-Yosida (RKKY) interaction between the localized spins which is mediated by the mobile conduction electrons. In such a scenario, the Heisenberg coupling $J_H \propto \rho_0 J_K^2$, where ρ_0 is the density of states of the conduction electrons at the Fermi level. However, for the purpose of the present study, it is convenient to consider J_H as a parameter independent of J_K. Microscopically this can be justified by noting that, in principle, there can be other sources which generate this coupling, such as superexchange within the narrow band of f electrons.

In order to perform a systematic large N study[28] of the system defined by Eqs. (1) and (2), the first step is to decouple the interaction terms which are quartic in fermionic operators using a Hubbard-Stratonovich transformation. The Heisenberg exchange term is decoupled using a bosonic link variable $\phi_{ij} \rightarrow \Sigma_{\alpha} f_{i\alpha}^{\dagger} f_{j\alpha}$, while the Kondo interaction is decoupled by introducing a complex bosonic field $\sigma_i^{\dagger} \rightarrow \Sigma_{\alpha} f_{i\alpha}^{\dagger} c_{i\alpha}$. In the next step, following Ref. 15, we assume that in three dimensions, ϕ_{ij} condenses in a uniform spin liquid phase, i.e., $\langle \phi_{ij}\rangle = \phi_0$ at the mean-field level.[29] This provides a dispersion to the spinon band which, as we will show later, is an essential ingredient to obtain the breakdown of the Kondo effect. We note that there is no clear evidence of a spin liquid phase in any heavy fermion system near its quantum critical point. Rather, the typical phase diagram exhibits a QCP that separates a magnetic ground state (typically an antiferromagnet) from a paramagnetic heavy Fermi liquid. Consequently, it is useful to discuss the motivation for our choice of a uniform spin liquid phase for the Heisenberg link variable ϕ_{ij}. This choice is partly guided by convenience: since our main purpose is to study the consequences of the breakdown of the Kondo effect, the choice of a uniform spin liquid can be viewed as the simplest device which allows the vanishing of the Kondo energy scale (indicating the breakdown of the Kondo effect) at the mean-field level.[29] More physically, one can view the uniform spin liquid as a mean-field description of the short-range magnetic correlations that persist when a magnetic ground state is destroyed by quan-

tum fluctuations. However, to demonstrate this point concretely is not simple and beyond the scope of the present study. The key point is that the spin liquid provides a bandwidth for the f electrons. Other approaches, for instance, one where the bandwidth is due to direct f-f hopping, should yield similar results with regards to the breakdown of the Kondo effect that we describe here.

The system can now be described by the Lagrangian,[16,30]

$$\mathcal{L} = \sum_{\langle ij\rangle\alpha} \{c_{i\alpha}^{\dagger}(\partial_\tau \delta_{ij} - t)c_{j\alpha} + f_{i\alpha}^{\dagger}[(\partial_\tau - \lambda_i)\delta_{ij} - \phi_0 e^{ia_{ij}}]f_{j\alpha}\} + \frac{N}{2}\sum_i \lambda_i + \frac{N}{J_K}\sum_i \sigma_i^{\dagger}\sigma_i + \frac{N\phi_0^2}{J_H} + \sum_{i\alpha}(c_{i\alpha}^{\dagger} f_{i\alpha}\sigma_i + \text{H.c.}), \tag{3}$$

where V (the volume of the system) is set to 1. In the above, λ_i are Lagrange multipliers (scalar potential) that enforce the local constraint of $N/2$ spinons per site. Now, given a many-body wave function that satisfies this constraint, a single hop of a spinon takes the state out of the physical subspace. Consequently, for the kinematics of the spinons, only simultaneous opposite hops between two neighboring sites are physically allowed process. This implies that the local spinon current operator $\vec{J}_{fi}=0$ at every site i. The gauge fields a_{ij} (vector potential), associated with the phase of ϕ_{ij}, ensure that this constraint is satisfied. The appearance of the scalar and vector potentials can also be understood by noting that $\mathcal{L}$ is invariant (up to a term which is a total derivative of imaginary time) under a local U(1) gauge transformation $f_{i\alpha} \to f_{i\alpha}e^{i\theta_i}$, $\sigma_i \to \sigma_i e^{-i\theta_i}$, $\lambda_i \to \lambda_i + i\partial_\tau\theta_i$, and $a_{ij} \to a_{ij} - \theta_i + \theta_j$, a consequence of the fermionic representation of the spin and the constraint [Eq. (2)].[31]

In the following we examine the above Lagrangian, first in a mean-field approximation, and then consider Gaussian fluctuations of the action around the mean-field solution. This involves studying the possibility of hybridization between the conduction and the spinon bands (for $\langle\sigma_i\rangle \neq 0$) as well as calculating the hybridization fluctuation which is an interband particle-hole excitation. As such, one needs to characterize the dispersions of the conduction and the spinon bands. We do this by assuming that the bands have a parabolic dispersion (to facilitate calculations), and we introduce the following two important parameters. First, $\alpha \equiv \phi_0/D$ is the ratio of the spinon bandwidth ϕ_0 and the conduction bandwidth D. As we will see in Sec. III, at the Kondo breakdown QCP $\phi_0 \sim J_H \sim T_K^0$, where $T_K^0 \equiv De^{-1/(\rho_0 J_K)}$ is the single-ion Kondo energy scale of the system, which is typically of order 10 K in heavy fermion systems. Assuming $D \sim 10^4$ K, we get $\alpha \sim 10^{-3}$. Second, while the spinon band is half filled due to the constraint (for $N=2$), the conduction-band filling is generic. Without any loss of generality, we take the conduction band to be less than half filled. This implies that the Fermi wave vector of the conduction band k_F is different from that of the spinon band k_{F0}. We denote this mismatch by $q^* \equiv k_{F0} - k_F$ and assume that the fraction (q^*/k_F) is of the order 0.1.[32] This would mean that while k_F and k_{F0} are of the order of the Brillouin-zone dimension, the mismatch wave vector q^* is 1 order of magnitude smaller.

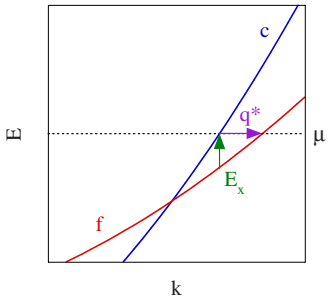

FIG. 1. (Color online) Dispersion of conduction and spinon bands, with the mismatch wave vector, q^*, and the mismatch energy, $E_x \equiv \alpha v_F q^*$, indicated, where α is the ratio of the spinon and conduction bandwidths. An artificially large value of α was used in this plot (0.5) so as to better illustrate the origin of E_x.

The parameters α and (q^*/k_F) affect the important energy scales of the system. This is illustrated in Fig. 1 where we show the conduction and spinon dispersions.

III. MEAN-FIELD TREATMENT

At the level of the mean-field approximation, we replace the bosonic Hubbard-Stratonovich fields and the Lagrange multipliers by their expectation values, and we study the approximate Lagrangian given by

$$\mathcal{L}_{\text{MF}} = \sum_{\langle ij\rangle\alpha} \{c_{i\alpha}^{\dagger}(\partial_\tau \delta_{ij} - t)c_{j\alpha} + f_{i\alpha}^{\dagger}[(\partial_\tau - \langle\lambda_i\rangle)\delta_{ij} - \phi_0]f_{j\alpha}\} + \frac{N}{2}\sum_i \langle\lambda_i\rangle + \frac{N}{J_K}\sum_i |\langle\sigma_i\rangle|^2 + \frac{N\phi_0^2}{J_H} + \sum_{i\alpha}(c_{i\alpha}^{\dagger} f_{i\alpha}\langle\sigma_i\rangle + \text{H.c.}). \tag{4}$$

In the following we write the dispersion $(\epsilon_{\mathbf{k}})$ of the conduction band as

$$\epsilon_{\mathbf{k}} = \epsilon + \frac{\epsilon^2}{D}, \tag{5}$$

where $\epsilon = v_F(k - k_F)$, k is the magnitude of $\mathbf{k}$, and v_F is the Fermi velocity of the conduction electrons. The dispersion $(\epsilon_{\mathbf{k}}^0)$ of the spinon band is similarly written as

$$\epsilon_{\mathbf{k}}^0 = \alpha\left[(\epsilon - v_F q^*) + \frac{(\epsilon - v_F q^*)^2}{D}\right]. \tag{6}$$

We note that, in the above, both the bands are taken as electronlike, for which we find that the mean-field equations yield a spatially uniform solution, namely, $\langle\sigma_i\rangle = \sigma_0$ and $\langle\lambda_i\rangle = \lambda_0$. In the case where one of the bands is chosen to be holelike, we find a spatially modulated solution[25] which we discuss in Appendix A 1. The free energy corresponding to Eq. (4) is given by

$$\frac{F_{\mathrm{MF}}}{N} = -\frac{1}{\beta}\mathrm{Tr}\{\ln[-G_a^{-1}(i\omega_n,\mathbf{k})] + \ln[-G_b^{-1}(i\omega_n,\mathbf{k})]\} + \frac{\sigma_0^2}{J_K} + \frac{\phi_0^2}{J_H} + \frac{\lambda_0}{2}, \tag{7}$$

where β is the inverse temperature, ω_n is the fermionic Matsubara frequency, and Tr corresponds to a trace over space-time coordinates. In the above

$$G_{a,b}^{-1}(i\omega_n,\mathbf{k}) = i\omega_n - \epsilon_{\mathbf{k}}^{a,b}, \tag{8}$$

where

$$\epsilon_{\mathbf{k}}^{a,b} = \frac{1}{2}[\epsilon_{\mathbf{k}} + \epsilon_{\mathbf{k}}^0 \mp \sqrt{(\epsilon_{\mathbf{k}} - \epsilon_{\mathbf{k}}^0)^2 + 4\sigma_0^2}]. \tag{9}$$

We evaluate the free energy given by Eq. (7) at zero temperature ($T=0$) in the limit $(q^*/k_F)\to 0$. The detail of this evaluation is given in Appendix A 2. As a function of α and σ_0 and to $\mathcal{O}(\sigma_0^4)$ accuracy, we find ($\alpha \ll 1$)

$$\frac{F_{\mathrm{MF}}}{N} = \frac{\rho_0 D^2}{2}\left[\frac{\alpha^2}{2\rho_0 J_H} - \frac{\alpha}{3}\right] + \rho_0\sigma_0^2\left[\frac{1}{\rho_0 J_K} - \ln\left(\frac{1}{\alpha}\right)\right] + \frac{\rho_0\sigma_0^4}{\alpha^2 D^2} + \mathrm{const}, \tag{10}$$

where the constant part has explicit λ_0 dependence. Since the precise value of λ_0 is of no importance for our results, in the following we ignore the mean-field equation for λ_0. Minimizing F_{MF} with respect to α and σ_0 we get

$$\frac{\rho_0 D^2}{2}\left[\left(\frac{\alpha}{\rho_0 J_H} - \frac{1}{3}\right) + \frac{2\sigma_0^2}{\alpha D^2} - \frac{4\sigma_0^4}{\alpha^3 D^4}\right] = 0, \tag{11}$$

$$2\rho_0\sigma_0\left\{\left[\frac{1}{\rho_0 J_K} - \ln\left(\frac{1}{\alpha}\right)\right] + \frac{2\sigma_0^2}{\alpha^2 D^2}\right\} = 0, \tag{12}$$

respectively. We study these equations by keeping the Heisenberg parameter J_H fixed, while varying the Kondo parameter J_K, and find two solutions corresponding to two mean-field ground states. (i) First, a uniform spin liquid phase where $\sigma_0=0$, which implies that in this phase, the Kondo effect fails to occur and the localized spins remain unscreened in a uniform spin liquid state. In this phase, $\alpha = \alpha_0 \equiv (\rho_0 J_H)/3$, which implies that the Heisenberg coupling sets the scale for the spinon dispersion, since $\phi_0 = (\rho_0 D J_H)/6 \sim J_H$. It is simple to check that this solution is stable for $J_K < J_{K_c}$, where

$$\frac{1}{\rho_0 J_{K_c}} = \ln\left(\frac{1}{\alpha}\right). \tag{13}$$

(ii) For $J_K > J_{K_c}$ the stable mean-field solution corresponds to $\sigma_0 \neq 0$, indicating a ground state where the local moments are screened by the Kondo effect and a heavy Fermi liquid is established below an energy scale $T_K \approx \pi\rho_0\sigma_0^2$. The growth of the Kondo order parameter in this phase is given by

$$\sigma_0 \propto J_H \ln\left(\frac{1}{\alpha_0}\right)\left[\frac{J_K - J_{K_c}}{D}\right]^{\beta}, \tag{14}$$

where $\beta = 1/2$ is the typical mean-field exponent. We also find that the spin liquid order parameter decreases in this phase and is given by

$$\alpha = \alpha_0 - \frac{6\sigma_0^2}{D^2} + \mathcal{O}(\sigma_0^4). \tag{15}$$

Thus, from the above mean-field study, we find that, in the presence of a finite bandwidth of the spinons, the Kondo effect takes place only when the Kondo coupling J_K is larger than a finite value J_{K_c}. This establishes the Kondo breakdown QCP where the lattice Kondo energy scale T_K vanishes. In the current formulation of the mean-field theory, the Kondo breakdown QCP separates a uniform spin liquid ground state ($J_K < J_{K_c}$) from a heavy Fermi-liquid ground state ($J_K > J_{K_c}$). It is important to note that if we define a single-ion Kondo scale (T_K^0) as a function of J_K for the system by

$$T_K^0(J_K) \equiv D e^{-1/(\rho_0 J_K)}, \tag{16}$$

using Eq. (13) we conclude that at the QCP

$$J_H \sim T_K^0(J_{K_c}). \tag{17}$$

This shows that the Kondo breakdown QCP is established as a result of a competition between the Kondo energy scale and the magnetic energy scale, even though there is no long-range magnetic order in the present study. The reduction in the spin liquid order parameter, given by Eq. (15), provides further evidence for this competition. Therefore, this mean-field study can be viewed as a microscopic realization of the energetic argument that Doniach[33] proposed several decades ago for the existence of a QCP in heavy fermion systems.

IV. FLUCTUATIONS

In this section, we study the massless fluctuations in the quantum critical regime. There are two such modes: (a) one associated with the phase of ϕ_{ij} which are the gauge fluctuations and (b) the fluctuations of the complex order parameter $(\sigma_i^\dagger, \sigma_i)$ which are gapless due to the vanishing of the Kondo energy scale T_K at the Kondo breakdown QCP.

A. Gauge fluctuations

Since the gauge fluctuations of the system have been studied earlier,[15] here we just summarize the main points for the sake of completeness. It is convenient to work in the Coulomb gauge $\vec{\nabla}\cdot\vec{a}=0$, where the vector gauge fields a_μ ($\mu = x,y,z$) are purely transverse.[31] In this gauge the fluctuations of the scalar potential λ decouple from a_μ and give rise to a screened Coulomb interaction between the spinons which can be neglected. Next, since the fields a_μ enter the theory as vectorial Lagrange multipliers to satisfy the constraint that the local spinon current is zero, they behave as "artificial photons" without any intrinsic dynamics of their own. Their dynamics is entirely generated by their coupling to the matter field, namely, the spinon band, and therefore

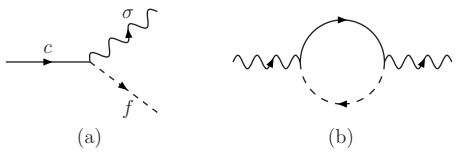

FIG. 2. (a) Vertex for the interaction between the conduction electrons (solid line) and the spinons (dashed line) mediated by the hybridization fluctuations σ (wiggly line). (b) The interband polarization involving conduction electrons and spinons, which generates the dynamics of σ. For momentum transfer $q>q^*$, where q^* is the mismatch between the conduction and the spinon Fermi surfaces, σ is an overdamped critical mode with dynamical exponent $z=3$.

these bosonic modes are overdamped. The propagator for the transverse gauge fields is defined as $D_{\mu\nu}(\mathbf{x},\tau)=\langle T_\tau[a_\mu(\mathbf{x},\tau)a_\nu(0,0)]\rangle$, which in frequency-momentum space has the standard form $D_{\mu\nu}(\mathbf{q},i\Omega_n)=(\delta_{\mu\nu}-q_\mu q_\nu/q^2)\Pi^{-1}(q,i\Omega_n)$, with $\Pi(q,i\Omega_n)\propto[(q/2k_{F0})^2+|\Omega_n|/(\alpha v_F q)]$. Here Ω_n is a bosonic Matsubara frequency, and the above expression for the gauge propagator $D_{\mu\nu}(\mathbf{q},i\Omega_n)$ is valid for frequencies smaller than the spinon bandwidth αD. As a result, the gauge excitations are characterized by a dynamical exponent $z=3$, which in $d=3$ are known[34] to give a contribution to the specific-heat coefficient $\gamma\equiv-\partial^2F/\partial T^2\propto\ln(\alpha D/T)$ and to the static spin susceptibility $\delta\chi_s\propto T^2\ln(\alpha D/T)$. Finally, it has been argued in the literature that the gauge fluctuations convert the finite temperature mean-field phase-transition line into a crossover line.[15,35]

B. Fluctuations of the Kondo boson

At the QCP, where the Kondo coupling is tuned to its critical value J_{K_c}, the critical fluctuations of the continuous phase transition are given by those of the complex order-parameter fields $(\sigma^\dagger,\sigma)$. The propagator for these fluctuations is defined by $D_\sigma(x,\tau)=\langle T_\tau[\sigma^\dagger(x,\tau)\sigma(0,0)]\rangle$. We get $D_\sigma^{-1}(\mathbf{q},i\Omega_n)=1/J_K+\Pi_{fc}(\mathbf{q},i\Omega_n)$, where

$$\Pi_{fc}(\mathbf{q},i\Omega_n)=\frac{1}{\beta}\sum_{\mathbf{k},i\omega_n}G_c(\mathbf{k},i\omega_n)G_f(\mathbf{k}+\mathbf{q},i\omega_n-i\Omega_n) \tag{18}$$

is the interband polarization bubble between the conduction and the spinon bands (Fig. 2). In the above $G_c^{-1}(\mathbf{k},i\omega_n)=(i\omega_n-\epsilon_\mathbf{k})$ is the propagator for the conduction electrons, while $G_f^{-1}(\mathbf{k},i\omega_n)=(i\omega_n-\epsilon_\mathbf{k}^0)$ is the propagator for the dispersive spinons. We write $\Pi_{fc}(\mathbf{q},i\Omega_n)=\Pi_{fc}(\mathbf{q},0)+\Delta\Pi_{fc}(\mathbf{q},i\Omega_n)$, where $\Pi_{fc}(\mathbf{q},0)$ is the static part of the fluctuations and $\Delta\Pi_{fc}(\mathbf{q},i\Omega_n)$ is the dynamic part. We first compute the static part which can be written as

$$\Pi_{fc}(\mathbf{q},0)=\sum_\mathbf{k}\frac{n_F(\epsilon_\mathbf{k})-n_F(\epsilon_{\mathbf{k}+\mathbf{q}}^0)}{\epsilon_\mathbf{k}-\epsilon_{\mathbf{k}+\mathbf{q}}^0}, \tag{19}$$

where $n_F(\epsilon)$ is the Fermi function. We find that $\Pi_{fc}(\mathbf{q},0)$ is independent of momentum if the dispersions are linearized in Eq. (19). This implies that the momentum dependence is due to $k\sim k_F$ in the $\mathbf{k}$ integral of Eq. (19), for which it is important to retain the quadratic dispersions of the bands. Furthermore, since the main contribution is for $k\sim k_F$, the small momentum scale q^* is unimportant and can be set to zero to facilitate the calculation, and we write $\epsilon_\mathbf{k}=(k^2-k_F^2)/(2m)$ and $\epsilon_\mathbf{k}^0=(k^2-k_F^2)/(2m_0)$. Then, in terms of α, the ratio of the two bandwidths that we introduced earlier, we have $\alpha=m/m_0$. Using $\mathbf{k}\leftrightarrow\mathbf{k}+\mathbf{q}$ inside the $\mathbf{k}$ summation we get

$$\begin{aligned}\Pi_{fc}(\mathbf{q},0)&=\sum_{k\le k_F}\left\{\frac{1}{\epsilon_\mathbf{k}-\epsilon_{\mathbf{k}+\mathbf{q}}^0}-\frac{1}{\epsilon_{\mathbf{k}+\mathbf{q}}-\epsilon_\mathbf{k}^0}\right\}\\&=\int_0^{k_F}\frac{dkk^2}{4\pi^2}\int_{-1}^{1}dz\left\{\frac{1}{B-\frac{qkz}{m}}-\frac{1}{C+\frac{qkz}{m_0}}\right\}\\&=\int_0^{k_F}\frac{dkk}{4\pi^2q}\left[m\ln\left|\frac{B+qk/m}{B-qk/m}\right|\right.\\&\quad\left.-m_0\ln\left|\frac{C+qk/m_0}{C-qk/m_0}\right|\right],\end{aligned}$$

where $B=A(k_F^2-k^2)-q^2/(2m)$, $C=A(k_F^2-k^2)-q^2/(2m_0)$, and $A=[1/(2m)-1/(2m_0)]$. After performing the momentum integration, we expand the resulting expression in powers of (q/k_F), and we use $\rho_0=mk_F/(2\pi^2)$, the density of states per spin of the conduction electrons at the Fermi level. To leading order in (q/k_F) we get

$$\begin{aligned}\Pi_{fc}(\mathbf{q},0)&=\rho_0\left[\frac{\ln\alpha}{(1-\alpha)}+\frac{1-\alpha^2+2\alpha\ln\alpha}{4(1-\alpha)^3}\left(\frac{q}{k_F}\right)^2\right]\\&\approx\rho_0\left[-\ln\left(\frac{1}{\alpha}\right)+\frac{q^2}{4k_F^2}\right].\end{aligned} \tag{20}$$

Note that the $\rho_0\ln(\alpha)$ term in the above equation has been derived in Appendix A 2 using a slightly different method for the calculation of the mean-field free energy in Eq. (10). This term along with $1/J_K$ define the mass $[1/J_K+\rho_0\ln(\alpha)]$ of the Kondo boson, which goes to zero at the QCP.

Next we calculate the dynamic part of the fluctuations which can be written as

$$\begin{aligned}\Delta\Pi_{fc}(\mathbf{q},i\Omega_n)=\Pi_{fc}(\mathbf{q},i\Omega_n)-\Pi_{fc}(\mathbf{q},0)=\frac{1}{\beta}\sum_{\mathbf{k},\omega_n}G_c(\mathbf{k},i\omega_n)\\\times[G_f(\mathbf{k}+\mathbf{q},i\omega_n-i\Omega_n)-G_f(\mathbf{k}+\mathbf{q},i\omega_n)].\end{aligned} \tag{21}$$

Unlike in the case of the static part, here the dominant contribution is from the interband particle-hole excitations around the two Fermi surfaces, for which the spectra can be linearized. We write $\epsilon_\mathbf{k}=\epsilon$ for the dispersion of the conduction electrons and $\epsilon_{\mathbf{k}+\mathbf{q}}^0=\alpha(\epsilon-v_Fq^*+v_Fqz)$ for the dispersion of the spinons, where z is the cosine of the angle between wave vectors $\mathbf{k}$ and $\mathbf{q}$. Approximating the $\mathbf{k}$ summation by

$$\sum_\mathbf{k}\rightarrow\frac{\rho_0}{2}\int_{-\infty}^{\infty}d\epsilon\int_{-1}^{1}dz,$$

at zero temperature we get

$$\Delta\Pi_{fc}(\mathbf{q},i\Omega_n) = \frac{\rho_0}{2(1-\alpha)}[Y_1 + Y_2 + Y_3 + Y_4], \quad (22a)$$

where

$$Y_{1,2} = \left(1 \mp \frac{E_1}{v_F q}\right)\ln(E_1 \mp v_F q), \quad (22b)$$

with $E_1 = v_F q^* - i\Omega_n/\alpha$ and

$$Y_{3,4} = -\left(1 \mp \frac{E_2}{v_F q}\right)\ln(E_2 \mp v_F q), \quad (22c)$$

with $E_2 = v_F q^* - i\Omega_n$. From the above expression of the dynamic part given by Eqs. (22a)–(22c), we next extract the leading behavior in different regimes of frequency and momentum. For this we need to compare the momentum q with q^*, and the frequency Ω_n (a continuous variable at $T=0$) with the energy scales $E_x \equiv \alpha v_F q^*$ and $\alpha v_F q$. Note that $v_F q^* \sim 10^3$ K is an energy scale much larger than the ultraviolet cutoff of the theory $\alpha D \sim 10$ K (the spinon bandwidth), and therefore we need to consider only $|\Omega_n| \ll v_F q^*$. We find five distinct regimes which are as follows: (i) $|\Omega_n| < E_x$ and $q < q^*$, where

$$\sum_i^4 Y_i \approx -2(1-\alpha)\frac{i\Omega_n}{E_x}\left[1 + \frac{1}{3}\left(\frac{q}{q^*}\right)^2 + \frac{1}{2}(1+\alpha)\frac{i\Omega_n}{E_x}\right]. \quad (23a)$$

Note that in the above, we retained two subleading terms because there are regimes where the subleading terms are larger than the static $(q/k_F)^2$ term. (ii) $|\Omega_n| < E_x$ and $q > q^*$, where

$$\sum_i^4 Y_i \approx -2(1-\alpha)\frac{i\Omega_n}{\alpha v_F q}\left[i\frac{\pi}{2}\mathrm{sgn}(\Omega_n) + \frac{q^*}{q}\right]. \quad (23b)$$

(iii) $|\Omega_n| > E_x$ and $q < q^*$, where

$$\sum_i^4 Y_i \approx 2\left[\ln\left(\frac{-i\Omega_n}{E_x}\right) + \frac{1}{6}\left(\frac{q}{q^*}\right)^2 - \frac{E_x}{i\Omega_n}\right]. \quad (23c)$$

(iv) $|\Omega_n| > \alpha v_F q > E_x$ and $q > q^*$, where

$$\sum_i^4 Y_i \approx 2\left[\ln\left(\frac{-i\Omega_n}{\alpha v_F q}\right) + 1 + i\frac{\pi}{2}\mathrm{sgn}(\Omega_n)\right]. \quad (23d)$$

(v) $\alpha v_F q > |\Omega_n| > E_x$ and $q > q^*$, where

$$\sum_i^4 Y_i \approx (1-\alpha)\frac{i\Omega_n}{\alpha v_F q}\left[-i\pi\,\mathrm{sgn}(\Omega_n) + (1+\alpha)\frac{i\Omega_n}{\alpha v_F q}\right]. \quad (23e)$$

At the quantum critical point, the mass of the Kondo boson goes to zero due to Eq. (13). The leading frequency and momentum dependences of $D_\sigma(\mathbf{q},i\Omega_n)$ are determined using Eqs. (20) and (22a). The details of the various asymptotic structures of $D_\sigma(\mathbf{q},i\Omega_n)$ in different regimes of frequency and momentum are discussed in Appendix B 1. Among the forms of $D_\sigma(\mathbf{q},i\Omega_n)$ given in Eqs. (B1a)–(B1c), (B2a)–(B2d), and (B3a)–(B3e), only the following two asymptotic structures are important for obtaining the leading contribution of the Kondo boson to thermodynamic and transport properties.

First, for $|\Omega_n| < [\alpha D/(2\pi)](q^*/k_F)^3$ and $q < q^*$, we get

$$D_\sigma^{-1}(\mathbf{q},i\Omega_n) \approx \rho_0\left[\frac{1}{4}\left(\frac{q}{k_F}\right)^2 - \frac{i\Omega_n}{E_x}\right], \quad (24)$$

which gives rise to an undamped propagating mode with dynamical exponent $z=2$ [the dispersion of which is given by setting Eq. (24) to zero]. The existence of this mode is a direct consequence of the mismatch between the Fermi surfaces of the conduction and the spinon bands. Due to this mismatch, a minimum momentum of q^* is necessary to excite an interband particle-hole pair. Consequently, for momentum $q < q^*$, the spectrum of the Kondo boson lies outside the continuum of the interband particle-hole excitations and thereby remains undamped. Note that this massless mode corresponds to hybridization fluctuations about the QCP and becomes massive for $J_K < J_{K_c}$ [this is realized by adding a constant term δ in Eq. (24)]. Since Π_{fc} at $q=0$ diverges logarithmically at E_x, the mode energy never exceeds E_x. The mode dispersion, which is quadratic about $q=0$, is more complicated as q approaches q^* due to logarithmic corrections to Π_{fc} and is described in greater detail in Appendix B 2.

Second, for most of the phase space, the spectrum for the fluctuations of σ lies within the interband particle-hole continuum, and we get

$$D_\sigma^{-1}(\mathbf{q},i\Omega_n) \approx \rho_0\left[\frac{1}{4}\left(\frac{q}{k_F}\right)^2 + \frac{\pi}{2}\frac{|\Omega_n|}{\alpha v_F q}\right], \quad (25)$$

i.e., an overdamped critical mode with dynamical exponent $z=3$. Next we note that, since we assume $q^* \ll k_F$, the overdamped $z=3$ critical mode occupies most of the momentum space and therefore almost always it provides the leading contribution to thermodynamic and transport properties. In this regime, the scaling of frequency is given by $\Omega_n \sim [(\alpha D)/(2\pi)](q/k_F)^3$, and since this regime ends for $q < q^*$, one obtains the infrared energy scale,

$$E^* \approx c\alpha D\left(\frac{q^*}{k_F}\right)^3, \quad (26)$$

where c is $1/(2\pi)$. The true value of c is slightly smaller (~ 0.1) since there are logarithmic corrections to Π_{fc} as q approaches q^*. A more detailed account is given in Appendix B 2. We note that E^* (which can be estimated to be ~ 1 mK for our choice of $q^* = 0.1k_F$) appears as an infrared crossover scale for any physical property that is affected by the excitations of σ. On the other hand, the ultraviolet cutoff scale is provided by $\alpha D \sim 10$ K, which is the bandwidth of the spinons or equivalently the single-ion Kondo scale by Eq. (17).

V. THERMODYNAMICS OF THE KONDO BOSON

In this section, we study the effect of the fluctuations of the Kondo boson σ on the thermodynamics of the system in the quantum critical regime. In particular, we compute (a) the

contribution to the free energy, (b) the temperature dependence of the static spin susceptibility, and (c) the crossover lines in temperature which demarcate the quantum critical regime.

A. Free energy

The contribution of the fluctuations of σ to the free energy (per unit volume) is given by

$$F = \sum_{\mathbf{q}} \int_{-\infty}^{\infty} \frac{d\Omega}{2\pi} \coth\left(\frac{\Omega}{2T}\right) \mathrm{Im}\ \ln[D_\sigma^{-1}(\mathbf{q}, \Omega + i\eta)], \quad (27)$$

where $D_\sigma(\mathbf{q}, \Omega + i\eta)$ denotes the retarded propagator for the Kondo bosons. We find that, for all temperatures $T < \alpha D$, the leading T dependence of the free energy F is given by that part of phase space where the mode is overdamped (with dynamical exponent $z=3$) and for which the expression for the propagator is approximately given by Eq. (25). The details of this demonstration, as well as the evaluation of the subleading contribution from the other regimes, are given in Appendix B 3. For $T > E^*$, the leading T dependence of F is given by

$$F \approx -\frac{k_F^3 \alpha D}{2\pi^3} \int_0^\infty d\Omega\ \coth\left(\frac{\Omega}{2T}\right) \int_{q_c}^1 dq q^2\ \tan^{-1}\left(\frac{2\pi\Omega}{q^3}\right). \quad (28)$$

Here q and q_c are dimensionless momenta in units of k_F and Ω and T are dimensionless energies in units of αD. Since the q integral is ultraviolet divergent, we use the Fermi momentum as an upper cutoff. The infrared cutoff, q_c, for the $z=3$ regime is dependent on the particular temperature range considered, since the leading T dependence comes from frequencies $\Omega \sim T$. For $T > E^*$, $q \gtrsim \Omega^{1/3}$, for which we can approximate $\tan^{-1}(x) \approx x$ and replace the cutoff q_c by $\Omega^{1/3}$. Performing the integrals, we find

$$F(T) \approx -\left(\frac{k_F^3}{9}\right) \ln\left(\frac{\alpha D}{T}\right) \frac{T^2}{\alpha D}, \quad T > E^*. \quad (29)$$

We note that this contribution adds to a similar $T^2\ \ln(T)$ contribution from the transverse gauge fluctuations (which are massless $z=3$ excitations). They give rise to a $\ln(T)$ behavior for the specific-heat coefficient.

For $T < E^*$, the leading contribution to the free energy is again given by Eq. (28) with $q_c = q^*/k_F$ for the infrared cutoff of the q integral. This is because for $\Omega \sim T < E^*$, the $z=3$ regime exists for $q > q^*$. As a result, because $\Omega^{1/3} < q^*/k_F$ in this temperature regime, the lower cutoff remains at q^*/k_F. This gives

$$F(T) \approx -\left(\frac{k_F^3}{3}\right) \ln\left(\frac{k_F}{q^*}\right) \frac{T^2}{\alpha D}, \quad T < E^*. \quad (30)$$

This T^2 dependence cannot be distinguished from ordinary Fermi-liquid corrections, and in this temperature regime the free energy is dominated by the $T^2\ \ln(T)$ contribution from the transverse gauge fluctuations.[34]

The collective mode gives a magnonlike contribution to the free energy ($F \sim T^{5/2}$) and is subleading relative to the $z=3$ contribution (see Appendix B 3). We illustrate this by showing in Fig. 3 a numerical determination of the contribution of the specific-heat coefficient, C/T, coming from the Kondo boson, using the fc polarization bubble of Eq. (22a). In this plot, one sees the subleading contribution arising from the $z=2$ region, the logarithmic contribution from the $z=3$ region which saturates for $T < E^*$, and the small difference between the positive and negative Ω contributions from the $z=3$ region due to the chirality of the fc polarization bubble.

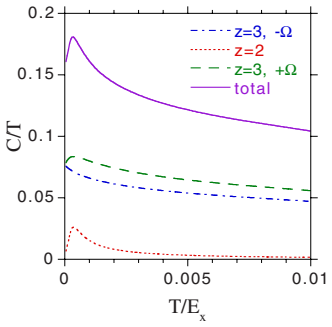

FIG. 3. (Color online) Numerical estimate of the contribution to the specific-heat coefficient, C/T, coming from the Kondo boson. Values of $\alpha = 0.001$ and $q^*/k_F = 0.1$ were assumed, with the momentum integral cutoff at k_F and the frequency integral at $0.1E_x$. Note the logarithmic behavior of the $z=3$ contribution which is cutoff for $T < E^*$ (with $E^* \sim 0.001E_x$) and the subleading nature of the $z=2$ contribution.

B. Static spin susceptibility

At the mean-field level, where the critical fluctuations of σ are ignored, the temperature dependence of the static spin susceptibility $\chi_s(T)$ is entirely analytic, namely, a constant (Pauli susceptibility) plus a T^2 term, which is usual for band fermions. Next, when we take the critical fluctuations into account, we expect the correction to $\chi_s(T)$ to be nonsingular (since the transition is nonmagnetic and the excitations of σ are in the singlet channel) but nonanalytic (due to the massless excitations). In order to evaluate this temperature dependence, we first need to compute $D_\sigma(\mathbf{q}, i\Omega_n)$ in the presence of a magnetic field (B). For a finite B, the effect of the Zeeman term is to shift the Fermi wave vectors k_F and k_F^0 of the conduction and the spinon bands, respectively. We get $k_F^0 \to k_F^0 \pm (\mu_B g_f B)/(\alpha v_F)$ and $k_F \to k_F \pm (\mu_B g_c B)/v_F$, where g_f and g_c are effective Landé g factors of the spinons and the conduction electrons, respectively, μ_B is the Bohr magneton, and $\pm$ refers to the up and down spins, respectively. Since $\alpha \ll 1$, and in general $g_f > g_c$, we can ignore the coupling of B to the c electrons and consider the effect of the Zeeman term as a renormalization of the mismatch wave vector q^*, which is given by

$$q^* \to q^* \pm \frac{\mu_B g_f B}{\alpha v_F}.$$

Next, we note that, in the presence of a finite q^*, one expects $\Pi_{fc}(0,0)$ to have corrections of the type q^*/k_F and $(q^*/k_F)^2$ [which are not calculated in Eq. (20), since the evaluation was performed in the limit $q^* \to 0$]. This implies that, in the

presence of a magnetic field, we expect a correction to $\Pi_{fc}(0,0)$ which is proportional to $[(\mu_B g_f B)/(\alpha D)]^2$ (since the excitation of σ is in the singlet channel, we do not expect a linear term in B). Adding such a term to $D_\sigma(\mathbf{q}, i\Omega_n)$ and noting that the leading temperature dependence is due to the overdamped $z=3$ mode, we can generalize Eq. (28) to obtain the B dependence of the free energy as

$$F(B,T) \approx -\frac{k_F^3 \alpha D}{2\pi^3}\int_0^\infty d\Omega \coth\left(\frac{\Omega}{2T}\right)\int_{q_c}^1 dq q^2 \times \tan^{-1}\left(\frac{2\pi\Omega}{q^3+h^2 q}\right). \tag{31}$$

Here energy and momenta are in dimensionless units [as in Eq. (28)] and $h=(\mu_B g_f B)/(\alpha D)$ is the dimensionless magnetic field. Writing the correction to the static spin susceptibility due to the fluctuations of σ as $\delta\chi_s(T) \equiv -[\partial^2 F/(\partial B)^2]_{B=0}$, we get for $T>E^*$

$$\delta\chi_s(T) \approx -(\mu_B g_f)^2\left[\frac{2^{4/3}\Gamma(4/3)\zeta(4/3)}{\pi^{5/3}3^{3/2}}k_F^3\right]\frac{T^{4/3}}{(\alpha D)^{7/3}}, \tag{32}$$

while for $T<E^*$, the lower cutoff is at q^*, making the mode effectively massive, and we get

$$\delta\chi_s(T) \approx -(\mu_B g_f)^2\left[\frac{1}{3}\frac{k_F^5}{(q^*)^2}\right]\frac{T^2}{(\alpha D)^3}. \tag{33}$$

As in the case of the free energy, the nonanalyticity in the leading temperature dependence is cutoff below E^* due to the mismatch wave vector q^*. As noted before, the gauge bosons give rise to a $T^2\ln(T)$ contribution to χ_s.

C. Crossover lines defining the quantum critical regime

The crossover lines in temperature that demarcate the quantum critical regime are symmetric about the QCP $\delta=\delta_c=0$, where $\delta=1/(\rho_0 J_K)-1/(\rho_0 J_{K_c})$ is the dimensionless tuning parameter of the theory (for fixed J_H). On the heavy Fermi-liquid side of the QCP, such a line usually defines the boundary of the finite temperature phase transition. However, it has been argued in the literature that the gauge fluctuations convert the finite temperature mean-field phase-transition line into a crossover line.[15,35] These lines are determined by the temperature dependent mass $\delta m(T)$ of the excitations of σ. In a Ginzburg-Landau approach, these excitations are generated by the quartic $u_0|\sigma|^4$ coupling in the action, where $u_0 \sim \rho_0/(\alpha D)^2$ from Eq. (10). In the following, we compute $\delta m(T)$ generated due to the propagating mode with $z=2$ given by Eq. (24), as well as that generated by the overdamped mode with $z=3$ given by Eq. (25). The contributions from the other regimes of $D_\sigma(\mathbf{q}, i\Omega_n)$ are always subleading. The general expression for $\delta m(T)$ is given by

$$\delta m(T) = u_0 \sum_{\mathbf{q}} \int_{-\infty}^{\infty}\frac{d\Omega}{2\pi}\coth\left(\frac{\Omega}{2T}\right)\mathrm{Im}\, D_\sigma(\mathbf{q}, \Omega + i\eta). \tag{34}$$

Denoting the contribution of the $z=2$ mode as $\delta m_1(T)$, we get using Eq. (24)

$$\delta m_1(T) = \left(\frac{u_0 E_x}{2\pi^2\rho_0}\right)\int_0^{q^*} dq q^2 n_B\left(\frac{E_x q^2}{4k_F^2}\right),$$

where $n_B(x)=(e^{x/T}-1)^{-1}$ is the Bose function. For the leading T dependence, we write $n_b(x)\approx 1/x$, with an appropriate ultraviolet cutoff for the q integral. For $T<E^*$, this cutoff is $k_F(T/E_x)^{1/2}$, and for $T>E^*$, this cutoff remains at q^*. We get

$$\delta m_1(T) \approx \left(\frac{4u_0 k_F^3}{\pi^2\rho_0}\right)\frac{T^{3/2}}{E_x^{1/2}}, \quad T<E^*,$$

$$\approx \left(\frac{2u_0 k_F^2 q^*}{\pi^2\rho_0}\right)T, \quad T>E^*. \tag{35}$$

Next, denoting the contribution of the $z=3$ mode as $\delta m_2(T)$, we get

$$\delta m_2(T) = \left(\frac{4u_0\alpha D k_F^3}{\pi^2\rho_0}\right)\int_0^\infty d\Omega \coth\left(\frac{\Omega}{2T}\right)\Omega \times \int_{q_c}^\infty dq \frac{q^3}{q^6+4\pi^2\Omega^2},$$

where q and q_c are dimensionless in units of k_F and Ω and T are dimensionless in units of αD. For $T>E^*$, we can set $q_c \sim \Omega^{1/3}$ for the leading term, while for $T<E^*$ we have $q_c=q^*$. This gives

$$\delta m_2(T) \approx \left[\frac{2u_0 k_F^3}{3\rho_0}\right]\left(\frac{k_F}{q^*}\right)^2\frac{T^2}{\alpha D}, \quad T<E^*,$$

$$\approx \left[\frac{2^{7/3}\Gamma(4/3)\zeta(4/3)u_0 k_F^3}{3^{3/2}\pi^{5/3}\rho_0}\right]\frac{T^{4/3}}{(\alpha D)^{1/3}}, \quad T>E^*. \tag{36}$$

Comparing Eqs. (35) and (36) we find that, for $T<E^*$, the leading T dependence is given by the $z=2$ mode and $\delta m(T)\approx\delta m_1(T)$, while for $T>E^*$, the leading term is from the $z=3$ damped mode and $\delta m(T)\approx\delta m_2(T)$. Consequently, the crossover lines in temperature which define the quantum critical regime are given by

$$T \propto |\delta-\delta_c|^{2/3}, \quad T<E^*,$$

$$\propto |\delta-\delta_c|^{3/4}, \quad T>E^*. \tag{37}$$

VI. QUASIPARTICLE LIFETIME AND TRANSPORT

In this section, we first evaluate the quasiparticle lifetime (τ_c) of the conduction electrons due to scattering from the excitations of σ and then argue that this lifetime can be identified with the transport lifetime (τ_{tr}) for the evaluation of the

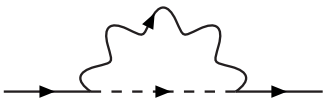

FIG. 4. Self-energy diagram for the conduction electrons due to scattering from the critical excitations of σ whose dynamical exponent is $z=3$. In three dimensions, this has a marginal Fermi-liquid form.

temperature dependence of the resistivity. For the process shown in Fig. 4, the general expression for the imaginary part of the self-energy of the conduction electrons is given by

$$\mathrm{Im}\,\Sigma_c^R(\mathbf{k},\omega) = \sum_{\mathbf{q}} \int_{-\infty}^{\infty} \frac{d\Omega}{\pi}[n_B(\Omega)+n_F(\Omega-\omega)] \times \mathrm{Im}\,D_\sigma^R(\mathbf{q},\Omega)\mathrm{Im}\,G_f^R(\mathbf{k}-\mathbf{q},\omega-\Omega), \tag{38}$$

where $n_F(x)=(e^{x/T}+1)^{-1}$ is the Fermi function and R denotes retarded functions. At zero temperature, this gives

$$\mathrm{Im}\,\Sigma_c^R(\mathbf{k},\omega) = \sum_{\mathbf{q}} \int_{0}^{\omega} \frac{d\Omega}{\pi}\mathrm{Im}\,D_\sigma^R(\mathbf{q},\Omega) \times \mathrm{Im}\,G_f^R(\mathbf{k}-\mathbf{q},\omega-\Omega). \tag{39}$$

We evaluate the above expression for a conduction electron on the Fermi surface, i.e., for $|\mathbf{k}|=k_F$, and we find that the leading frequency dependence is always due to the overdamped $z=3$ mode whose expression is given by Eq. (25). The $z=2$ mode does not contribute since it cannot kinematically connect the f and c electrons. We write

$$\sum_{\mathbf{q}} \rightarrow \frac{1}{4\pi^2}\int_0^\infty dq q^2 \int_{-1}^{1} dz,$$

where z is the cosine of the angle between $\mathbf{k}$ and $\mathbf{q}$. After linearizing the spectrum for the spinons, we have

$$\mathrm{Im}\,G_f^R(\mathbf{k}_F-\mathbf{q},\omega-\Omega) = -\pi\delta(\omega-\Omega+E_x+\alpha v_F q z).$$

Since, $\Omega\sim\omega$ and $q>q^*$ for the overdamped mode, the constraint from the δ function is always satisfied. After the angular integral, we get

$$\mathrm{Im}\,\Sigma_c^R(k_F,\omega) = -\left(\frac{2k_F^3}{\pi\rho_0}\right)\int_0^\omega d\Omega\Omega\int_{q^*}^{\infty} dq\frac{q^2}{q^6+4\pi^2\Omega^2},$$

where momenta and frequencies are dimensionless in units of k_F and αD, respectively. For $\Omega\sim\omega>E^*$, the leading contribution of the q integral comes from $q\sim(\Omega)^{1/3}$ and therefore the infrared cutoff q^* can be set to zero. However for $\Omega\sim\omega<E^*$, $q^*>\Omega^{1/3}$, and the lower cutoff at q^* comes into play. We finally get

$$\mathrm{Im}\,\Sigma_c^R(k_F,\omega) \approx -\left(\frac{k_F^3}{6\pi\rho_0\alpha D}\right)|\omega|, \quad |\omega|>E^*,$$

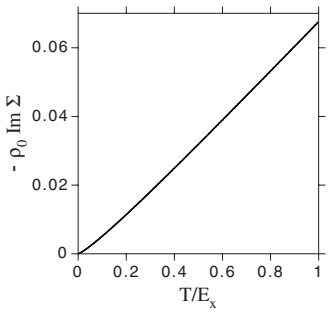

FIG. 5. The imaginary part of the conduction-electron self-energy at $\omega=0$ versus T from a numerical evaluation of Eq. (41) using Eq. (25). Note the approximate linear T behavior, with a crossover to T^2 behavior at very low T.

$$\approx -\left(\frac{k_F^3}{6\pi^2\rho_0\alpha D E^*}\right)\omega^2, \quad |\omega|<E^*. \tag{40}$$

Thus we find that above the infrared cutoff scale E^*, the Kondo breakdown scenario, in which the conduction electrons interact with the critical hybridization fluctuations, provides a microscopic mechanism to obtain a marginal Fermi liquid[36] in three dimensions.

Next we evaluate the temperature dependence of the imaginary part of the self-energy at $\omega=0$ and on the Fermi surface. Denoting this as $\mathrm{Im}\,\Sigma_c(T)$, we get from Eq. (38)

$$\mathrm{Im}\,\Sigma_c^R(T) = \sum_{\mathbf{q}} \int_{-\infty}^{\infty} \frac{d\Omega}{\pi}\frac{1}{\sinh(\Omega/T)}\mathrm{Im}\,D_\sigma^R(\mathbf{q},\Omega) \times \mathrm{Im}\,G_f^R(\mathbf{k}_F-\mathbf{q},-\Omega). \tag{41}$$

The evaluation of the above expression is very similar to the finite frequency case, except for $T>E^*$, the thermal factors $n_B(x)+n_F(x)=1/\sinh(x)$ gives an additional logarithm which is cutoff by E^*. We get

$$\mathrm{Im}\,\Sigma_c^R(T) \approx -\left(\frac{k_F^3}{3\pi\rho_0\alpha D}\right)T\ln\left(\frac{2T}{E^*}\right), \quad T>E^*,$$

$$\approx -\left(\frac{k_F^3}{6\rho_0\alpha D E^*}\right)T^2, \quad T<E^*. \tag{42}$$

In Fig. 5, we show a plot of this quantity from a numerical evaluation of Eq. (41) using Eq. (25). One can see the approximate linear T behavior except at very low temperatures, where one crosses over to a T^2 behavior.

Next we evaluate the temperature dependence of the resistivity $\delta\rho(T)\equiv\rho(T)-\rho(0)$. In order to proceed, we first need to address whether the transport lifetime τ_{tr} can be identified with the quasiparticle lifetime $\tau_c(\omega,T)\propto[\mathrm{Im}\,\Sigma_c(\omega,T)]^{-1}$, whose frequency and temperature dependences are given by Eqs. (40) and (42). For this, it is useful to compare the Kondo-Heisenberg model with a single band model. In the latter case, the two lifetimes have a different temperature dependence because the leading contribution to the self-energy comes from forward-scattering processes with momentum transfer $q\simeq 0$ but which are not effective in relaxing the current. As such, when vertex corrections are

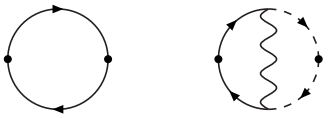

FIG. 6. Diagrams for the current-current correlator for the evaluation of the conductivity in the Kubo formalism. The solid dots indicate current vertices. (a) involves conduction electrons with self-energy corrections (see Fig. 4). This contribution identifies the transport lifetime with the conduction-electron lifetime. (b) Vertex correction involving the exchange of one σ boson. It vanishes because the spinon current is zero due to the local constraint [see Eq. (2)].

taken into account, $\tau_{\rm tr}^{-1}$ acquires an additional temperature dependence proportional to $q^2 \sim T^{2/z}$. However, this is not the case for the Kondo-Heisenberg model which has two bands, one of light conduction electrons and the other of heavy spinons. Due to the constraint of half filling [Eq. (2)], the spinon current operator $\vec{J}_{fi}=0$ at every site i. Therefore, it is guaranteed by gauge invariance that a vertex correction involving the exchange of a single σ boson [Fig. 6(b)], which involves an external spinon current operator, is identically zero.[37] The first nonzero vertex correction involves the exchange of two σ bosons, and we expect such a correction to be small by a factor of α. This can be understood as well in a Boltzmann approach,[38] where the transport vertex correction $1-\cos(\theta)$ gets replaced by $1-\alpha\cos(\theta)$, which is essentially unity since $\alpha \ll 1$.

Consequently, in the present theory, the transport lifetime is proportional to the quasiparticle lifetime. The physical picture that emerges from the above discussion is that, when scattered from a σ boson ($c \rightleftharpoons f+\sigma$), a conduction electron transmutes into a spinon and relaxes its current in the bath of the spinons. More formally, the expression for the conductivity (σ_c) obtained from the current-current correlator in the Kubo formalism is given by

$$\sigma_c = \left(\frac{v_F^2}{3}\right)\sum_{\mathbf{k}} \int_{-\infty}^{\infty} \frac{d\omega}{2\pi}\left[\frac{\partial}{\partial\omega}\tanh\left(\frac{\omega}{2T}\right)\right][\mathrm{Im}\, G_c^R(\mathbf{k},\omega)]^2. \tag{43}$$

We write

$$[G_c^R(\mathbf{k},\omega)]^{-1} = \omega - \epsilon_k - \mathrm{Re}\,\Sigma(\omega) + \frac{i}{2\tau_c(\omega,T)}, \tag{44}$$

where for $(\omega,T) > E^*$

$$[\tau_c(\omega,T)]^{-1} = \tau^{-1} + \left(\frac{2k_F^3}{3\pi\rho_0\alpha D}\right)\left[T\ln\left(\frac{2T}{E^*}\right) + \frac{|\omega|}{2}\right]. \tag{45}$$

Here τ is an elastic-scattering lifetime of the conduction electrons due to impurities and sets the scale of the temperature independent part of σ_c. We linearize the dispersion of the conduction electrons and replace the momentum sum by an energy integral, and we finally obtain $\sigma_c(T) = [\rho_0 v_F^2 \tau_c(0,T)]/3$. This implies for $E^* < T < \alpha D$,

$$\delta\rho(T) \propto T\ln\left(\frac{2T}{E^*}\right). \tag{46}$$

Therefore, the scenario of the breakdown of the Kondo effect captures one of the most enigmatic features of heavy fermion systems close to quantum criticality, namely, the quasilinear temperature dependence of the resistivity observed for most compounds over a large range of temperature. For $T < E^*$, the usual Fermi-liquid result is recovered and $\delta\rho(T) \propto T^2$. It is interesting to note that the recovery of the Fermi-liquid T^2 behavior of resistivity below a finite temperature scale in the quantum critical regime of $YbRh_2Si_2$ has recently been reported.[39] Finally, we note that for the same reason that equates the single-particle and transport lifetimes, the electrical and thermal transport lifetimes are the same.

VII. CONCLUSION

To summarize, we studied the Kondo-Heisenberg model in three dimensions using a fermionic representation for the localized spins. The mean-field phase diagram in the $T-J_K$ plane, where J_K is the Kondo coupling, exhibits a quantum critical point that separates a uniform spin liquid phase from a heavy Fermi-liquid phase. In the uniform spin liquid phase, the Kondo hybridization between the conduction band and the band of fermionic spinons that constitute the local moments vanishes, thereby indicating that in this phase, the Kondo effect fails to occur. For a Kondo coupling larger than the critical value ($J_K > J_{K_c}$), a heavy Fermi-liquid ground state is established with finite hybridization between the bands. This implies that at the quantum critical point ($J_K = J_{K_c}$), the lattice Kondo energy scale T_K vanishes, indicating the breakdown of the Kondo effect for couplings smaller than the finite value J_{K_c}.

In general, the size of the (hot) Fermi surface of the spinon band is different from that of the conduction electrons, and we characterized their mismatch by a wave vector $q^* \equiv k_{F0} - k_F$, where k_{F0} is the spinon Fermi wave vector and k_F is the conduction Fermi wave vector. As a consequence of this mismatch, we found that two mean-field solutions are possible in the Fermi-liquid phase. First, one with a uniform hybridization, which is stabilized when the two band masses have the same sign. This is the standard Kondo phase which appears in the mean-field pseudofermion description of the Kondo lattice. Second, a Kondo phase with the hybridization modulated in space with wave vector $q_0 \approx 1.2q^*$, which appears when the two band masses have opposite signs (i.e., one band is electronlike and the other holelike). Conceptually, this phase is analogous to the LOFF state of superconductivity and is characterized by nodes in space where T_K is zero. This solution was discussed at the mean-field level in Ref. 25 and Appendix A 1. Fluctuations in the modulated case are more complex than for the uniform case and will be the topic for future work. For the uniform case, we showed that at the quantum critical point the single-ion Kondo scale T_K^0 is approximately equal to the Heisenberg coupling J_H. This demonstrates that the Kondo breakdown is a consequence of the competition between the Kondo energy scale and the magnetic energy scale, even though there is no long-

range magnetic order in the present formulation.

Then, we studied the effect of the critical hybridization fluctuations (excitations of the order parameter σ) associated with the vanishing energy scale T_K on the thermodynamic and transport properties of the system. We found that, due to the mismatch q^*, the critical fluctuations are affected by energy scales $E^* \sim [\alpha D/(2\pi)](q^*/k_F)^3$ and $E_x \sim \alpha v_F q^*$, where $\alpha \sim J_H/D$ is the ratio of the spinon bandwidth J_H and the conduction bandwidth D. The propagator for the critical modes has several asymptotic structures in different regimes of frequency-momentum space, out of which the following two are important and readily understood. (i) For momentum $q < q^*$, the spectrum of the critical fluctuations lies outside the interband particle-hole continuum and therefore their dynamics is undamped and is characterized by a dynamical exponent $z=2$. (ii) For most of momentum space ($q > q^*$), the spectrum of the critical modes lies within the particle-hole continuum and therefore has overdamped dynamics with exponent $z=3$ (Landau damping). The leading contribution to thermodynamics and transport is almost always governed by the latter asymptotic structure, in contrast to most Ginzburg-Landau approaches, where only the critical modes within $1/\xi(T)$ of the ordering vector ($q=0$) are important.[40] Above the temperature scale E^*, this gives rise to anomalous metallic behavior, such as a specific-heat coefficient that diverges logarithmically with temperature, and the inverse lifetime of the conduction electrons which has a $T \ln T$ temperature dependence. The latter is a consequence of the conduction-electron scattering with the critical bosons with the dynamical exponent $z=3$, which in three dimensions provide a microscopic mechanism to obtain marginal Fermi-liquid behavior. Since the spinons do not carry current but are effective in relaxing the current carried by the conduction electrons, the T dependence of the inverse particle lifetime also gives rise to a $T \ln T$ behavior of the resistivity. From a scaling point of view, in this regime the frequency Ω of the critical fluctuations scales as $\Omega \sim q^3$, where q is their momentum. For $T < E^*$, however, the infrared cutoff q^* prohibits the $z=3$ scaling, and the leading T dependence of the specific-heat coefficient and the resistivity are Fermi-liquid-like. The Kondo breakdown scenario is promising in that it can explain one of the least understood features of the heavy fermions near quantum criticality, namely, the quasilinear temperature dependence of the resistivity and the existence of multiple energy scales over decades of temperature.

ACKNOWLEDGMENTS

We thank the hospitality of the KITP where this work was initiated. We also acknowledge J. Schmalian, P. Sharma, A. Chubukov, P. Coleman, G. Kotliar, M. Civelli, and L. De Leo for illuminating discussions. This work was supported by the U.S. Department of Energy, Office of Science, under Contract No. DE-AC02-06CH11357, in part by the National Science Foundation under Grant No. PHY99-07949, and by the French ANR Program under Grant No. ANR36ECCEZZZ.

APPENDIX A

1. Spatially modulated mean-field solution

Here we demonstrate that when the conduction electron and spinon masses have opposite signs, i.e., when one band is electronlike and the other holelike, the mean-field theory admits a solution where the Kondo hybridization is modulated in space. This is a consequence of the mismatch between the two Fermi surfaces and conceptually is analogous to the LOFF state of superconductivity.[22,23] In the following, we choose the conduction band to be electronlike and the spinon band to be holelike and linearize their dispersions. This gives $\epsilon_{\mathbf{k}} = \epsilon$ for the dispersion of the conduction band, where $\epsilon = v_F(k - k_F)$ and $\epsilon^0_{\mathbf{k}} = -\alpha(\epsilon - v_F q^*)$ for the dispersion of the spinon band. For this case, we evaluate the static interband polarization $\Pi_{fc}(\mathbf{q},0)$, whose general expression is given by Eq. (19). Approximating the momentum summation by

$$\sum_{\mathbf{k}} \rightarrow \frac{\rho_0}{2} \int_{-D}^{D} d\epsilon \int_{-1}^{1} dz,$$

where the conduction bandwidth D enters as an ultraviolet cutoff for the energy integral, we get

$$\Pi_{fc}(\mathbf{q},0) = \frac{\rho_0}{1+\alpha} \left\{ \ln\left[\frac{\alpha v_F^2 |(q^*)^2 - q^2|}{(1+\alpha)^2 D^2} \right] - 2 + \frac{q^*}{q} \ln\left[\frac{q^* + q}{|q^* - q|} \right] \right\}. \tag{A1}$$

It is easy to see that the maximum of $-\Pi_{fc}(\mathbf{q},0)$ is at a finite wave vector q_0 where

$$q_0 \approx 1.2 q^*. \tag{A2}$$

Therefore for $J_K > J_{K_c}$, where the critical value of the Kondo coupling is given by

$$\frac{1}{J_{K_c}} + \Pi_{fc}(q_0,0) = 0,$$

the Kondo boson condenses in the Fermi-liquid phase at a finite wave vector q_0 (i.e., $\langle \sigma_{q_0} \rangle \neq 0$). This implies that the Kondo hybridization is modulated, with nodes in space where T_K vanishes.[41]

2. Calculation of the mean-field free energy

In this part, we give the technical details for the evaluation of the mean-field free energy at $T=0$. This can be written as

$$\frac{F_{\mathrm{MF}}}{N} = \sum_{\mathbf{k},i=a,b} \epsilon^i_{\mathbf{k}} \theta(-\epsilon^i_{\mathbf{k}}) + \frac{\sigma_0^2}{J_K} + \frac{\phi_0^2}{J_H} + \frac{\lambda_0}{2}, \tag{A3}$$

where $\theta(x)$ is the Heaviside step function and $\epsilon^{a,b}_{\mathbf{k}}$ are given by Eq. (9). We replace $\Sigma_{\mathbf{k}} \rightarrow \rho_0 \int d\epsilon$, and from the solution of the equations $\epsilon^{a,b}_{\mathbf{k}} = 0$, we get

$$\sum_{\mathbf{k},i=a,b} \epsilon^i_{\mathbf{k}} \theta(-\epsilon^i_{\mathbf{k}}) = \frac{\rho_0}{2} \int_{-D}^{s-s_1} d\epsilon \left\{ (1+\alpha)\left(\epsilon + \frac{\epsilon^2}{D}\right) - \left[(1-\alpha)^2 \left(\epsilon + \frac{\epsilon^2}{D}\right)^2 + 4\sigma_0^2 \right]^{1/2} \right\} + \frac{\rho_0}{2} \int_{-D}^{-s-s_1} d\epsilon \left\{ (1+\alpha)\left(\epsilon + \frac{\epsilon^2}{D}\right) \right.$$

$$+\left[(1-\alpha)^2\left(\epsilon+\frac{\epsilon^2}{D}\right)^2+4\sigma_0^2\right]^{1/2}\Bigg\},$$

where $s=\sigma_0/\alpha^{1/2}$ and $s_1=\sigma_0^2/(2D)+\mathcal{O}(1/D^2)$. We expand the expression under the square root in powers of $(1/D)$ and keep terms up to $\mathcal{O}(1/D^2)$, since higher orders contribute to $\mathcal{O}(\sigma_0^6)$ and beyond which we neglect. Performing the ϵ integral to $\mathcal{O}(\sigma_0^4)$ accuracy we get

$$\frac{F_{\mathrm{MF}}}{N}=\frac{\rho_0 D^2}{2}\left[\frac{\alpha^2}{2\rho_0 J_H}-\frac{\alpha}{3}\right]+\rho_0\sigma_0^2\left[\frac{1}{\rho_0 J_K}-\frac{1}{1-\alpha}\ln\left(\frac{1}{\alpha}\right)\right]+\frac{\rho_0\sigma_0^4}{\alpha^2 D^2}\frac{(1-4\alpha+\alpha^2)}{(1+\alpha)},$$

where a constant part has been ignored. Since $\alpha\ll 1$, in the terms proportional to σ_0^2 and σ_0^4, we retain only the dominant α dependence and get Eq. (10).

APPENDIX B

1. Asymptotic structure of the Kondo boson

In this appendix, we determine the leading frequency and momentum dependences of the propagator for the Kondo boson $D_\sigma(\mathbf{q},i\Omega_n)$ in the quantum critical regime using Eqs. (20) and (22a). Its leading frequency dependence is given by the first terms in Eqs. (23a)–(23e), while the next term is determined by comparing the static $(q/k_F)^2$ term in Eq. (20) with the subleading terms of Eqs. (23a)–(23e). The asymptotic structure of $D_\sigma(\mathbf{q},i\Omega_n)$ in different regimes of frequency and momentum is as follows:

(1) $\Omega_n\ll E^*\equiv[(\alpha D)/(2\pi)](q^*/k_F)^3$. In this frequency interval there are three subregimes depending on the magnitude of the momentum $\mathbf{q}$. We get (a) $q\ll q_{\Omega 1}\equiv[\Omega_n/E_x]k_F$ (where $E_x\equiv\alpha v_F q^*$),

$$D_\sigma^{-1}(\mathbf{q},i\Omega_n)\approx-\rho_0\left(\frac{i\Omega_n}{E_x}\right)\left[1+\frac{1}{2}(1+\alpha)\frac{i\Omega_n}{E_x}\right], \quad \text{(B1a)}$$

(b) $q_{\Omega 1}\ll q\ll q^*$,

$$D_\sigma^{-1}(\mathbf{q},i\Omega_n)\approx\rho_0\left[\frac{1}{4}\left(\frac{q}{k_F}\right)^2-\frac{i\Omega_n}{E_x}\right], \quad \text{(B1b)}$$

and (c) $q^*\ll q\ll k_F$,

$$D_\sigma^{-1}(\mathbf{q},i\Omega_n)\approx\rho_0\left[\frac{1}{4}\left(\frac{q}{k_F}\right)^2+\frac{\pi}{2}\frac{|\Omega_n|}{\alpha v_F q}\right]. \quad \text{(B1c)}$$

(2) $E^*\ll\Omega_n\ll E_x$. In this frequency interval there are four subregimes given by (a) $q\ll q_{\Omega 2}\equiv(\Omega_n/E_x)^{1/2}q^*$,

$$D_\sigma^{-1}(\mathbf{q},i\Omega_n)\approx-\rho_0\left(\frac{i\Omega_n}{E_x}\right)\left[1+\frac{1}{2}(1+\alpha)\frac{i\Omega_n}{E_x}\right], \quad \text{(B2a)}$$

(b) $q_{\Omega 2}\ll q\ll q^*$,

$$D_\sigma^{-1}(\mathbf{q},i\Omega_n)\approx-\rho_0\left(\frac{i\Omega_n}{E_x}\right)\left[1+\frac{1}{3}\left(\frac{q}{q^*}\right)^2\right], \quad \text{(B2b)}$$

(c) $q^*\ll q\ll q_{\Omega 3}\equiv k_F[(q^*\Omega_n)/(\alpha k_F D)]^{1/4}$,

$$D_\sigma^{-1}(\mathbf{q},i\Omega_n)\approx-\rho_0\left(\frac{i\Omega_n}{\alpha v_F q}\right)\left[i\frac{\pi}{2}\mathrm{sgn}(\Omega_n)+\frac{q^*}{q}\right], \quad \text{(B2c)}$$

and (d) $q_{\Omega 3}\ll q\ll k_F$,

$$D_\sigma^{-1}(\mathbf{q},i\Omega_n)\approx\rho_0\left[\frac{1}{4}\left(\frac{q}{k_F}\right)^2+\frac{\pi}{2}\frac{|\Omega_n|}{\alpha v_F q}\right]. \quad \text{(B2d)}$$

(3) $E_x\ll\Omega_n\ll\alpha D$. In this frequency range there are five subregimes given by (a) $q\ll q_{\Omega 4}\equiv q^*(E_x/\Omega_n)^{1/2}$,

$$D_\sigma^{-1}(\mathbf{q},i\Omega_n)\approx\frac{\rho_0}{(1-\alpha)}\left[\ln\left(\frac{-i\Omega_n}{E_x}\right)-\frac{E_x}{i\Omega_n}\right], \quad \text{(B3a)}$$

(b) $q_{\Omega 4}\ll q\ll q^*$,

$$D_\sigma^{-1}(\mathbf{q},i\Omega_n)\approx\frac{\rho_0}{(1-\alpha)}\left[\ln\left(\frac{-i\Omega_n}{E_x}\right)+\frac{1}{6}\left(\frac{q}{q^*}\right)^2\right], \quad \text{(B3b)}$$

(c) $q^*\ll q\ll q_{\Omega 5}\equiv k_F[\Omega_n/(\alpha D)]$,

$$D_\sigma^{-1}(\mathbf{q},i\Omega_n)\approx\frac{\rho_0}{(1-\alpha)}\left[\ln\left(\frac{-i\Omega_n}{\alpha v_F q}\right)+1+i\frac{\pi}{2}\mathrm{sgn}(\Omega_n)\right], \quad \text{(B3c)}$$

(d) $q_{\Omega 5}\ll q\ll q_{\Omega 6}\equiv k_F[\Omega_n/(\alpha D)]^{1/2}$,

$$D_\sigma^{-1}(\mathbf{q},i\Omega_n)\approx\rho_0\left[\frac{\pi}{2}\frac{|\Omega_n|}{\alpha v_F q}-\frac{1}{2}(1+\alpha)\frac{\Omega_n^2}{(\alpha v_F q)^2}\right], \quad \text{(B3d)}$$

and (e) $q_{\Omega 6}\ll q\ll k_F$,

$$D_\sigma^{-1}(\mathbf{q},i\Omega_n)\approx\rho_0\left[\frac{1}{4}\left(\frac{q}{k_F}\right)^2+\frac{\pi}{2}\frac{|\Omega_n|}{\alpha v_F q}\right]. \quad \text{(B3e)}$$

2. Spectral response of the Kondo boson

In the paper, several simplified expressions were used for the spectral response of the Kondo boson. Here, we give a more complete account. The *fc* polarization bubble has some similarities to the Lindhard function[42] but also differs from it in important respects. In particular, the particle-hole continuum of the Lindhard function exists for all momenta, while this is not the case for the *fc* polarization as a result of the mismatch between the conduction and spinon Fermi surfaces. We have performed numerical calculations including the full quadratic dispersion of the fermions, but they are very similar to results we present here that are based on Eq. (22a) plus the static curvature correction [last term in Eq. (20)]. The advantage of using Eq. (22a) is that it is valid for arbitrarily small α. All results here are for the retarded response function at $T=0$. We confine our discussion to the case where both conduction and spinon bands have the same sign for the mass.

We begin with the *fc* bubble at $q=0$,

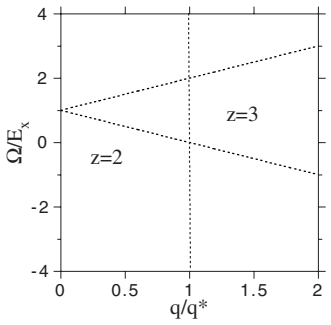

FIG. 7. Regimes of Π_{fc}. The various dashed lines are the kinematic lines corresponding to the zeros of the arguments of the logarithms in Eq. (22a). The regime denoted $z=2$ has $\mathrm{Im}\,\Pi_{fc}=0$, whereas the regime $z=3$ has $\mathrm{Im}\,\Pi_{fc}\propto\Omega$.

$$\mathrm{Re}\,\Pi_{fc}(0,\Omega)=\frac{\rho_0}{1-\alpha}\ln\frac{|\Omega-\alpha v_F q^*|}{|\Omega-v_F q^*|}. \tag{B4}$$

This expression contains two logarithmic singularities at the energies $E_x\equiv\alpha v_F q^*$ and $v_F q^*$, where $q^*\equiv k_{F0}-k_F$ is the mismatch vector between the conduction and spinon Fermi surfaces. The imaginary part of Π_{fc} is simply a step function with value $\pi\rho_0/(1-\alpha)$ between these two energies. Note that Π_{fc} is not symmetric around zero energy (only the sum of it with Π_{cf} would be). We have chosen $k_{F0}>k_F$. For the reverse case, the singularities would flip to the other side of the frequency axis. The logarithmic singularity at E_x plays an important role. It guaranties that the Kondo boson propagator, $D\equiv J_K/(1+J_K\Pi_{fc})$, always has a pole between zero and E_x. This pole is undamped since $\mathrm{Im}\,\Pi_{fc}$ is zero below E_x.

The general structure of Π_{fc} can be appreciated from Fig. 7, where the various domains for the imaginary part are shown. Note that the imaginary part vanishes in the regime we label as $z=2$. For the positive frequency side, this is a triangle in (q,Ω) space bounded by $(0,E_x)$ and $(q^*,0)$. For low frequencies appropriate for the dispersive peaks of $\mathrm{Im}\,D$, it will be sufficient to expand Eq. (22a) for small Ω. When we do this, we find

$$\mathrm{Re}\,D^{-1}=\delta-\frac{\rho_0\Omega}{2\alpha v_F q}\ln\frac{|q+q^*|}{|q-q^*|}+\frac{\rho_0 q^2}{4k_F^2}, \tag{B5}$$

where δ is the deviation from the quantum critical point (QCP) and the last term is the static curvature correction. Below the kinematic boundary, $\mathrm{Im}\,D^{-1}$ is zero, so the zeros of Eq. (B5) in this regime give the collective-mode dispersion, which for $\delta=0$ is

$$\Omega_{\mathrm{coll}}/E_x=0.5(q^*/k_F)^2(q/q^*)^3/\ln\frac{|q+q^*|}{|q-q^*|}. \tag{B6}$$

We compare this in Fig. 8 with the expression where the logarithm in Eq. (B5) is expanded for small q/q^*, the latter being Eq. (24). Note that formally, Eq. (B6) vanishes as q goes to q^*, but this is of no concern, since the mode intersects the kinematic boundary before this occurs, and thus it terminates at a finite energy, corresponding to $c\sim 0.1$ in Eq. (26).

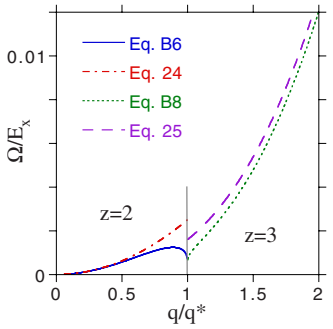

FIG. 8. (Color online) Dispersion of $\mathrm{Im}\,D$ for $\delta=0$ and $q^*/k_F=0.1$. The undamped ($z=2$) dispersion is to the left of the kinematic boundary, $\Omega/E_x=1-q/q^*$ (marked by the nearly vertical line), whereas the damped ($z=3$) response is to the right. The results based on Eq. (22a) closely follow the expressions of Eqs. (B6) and (B8). The simpler Eqs. (24) and (25) are used in the analytic calculations and are quite good except for q near q^*.

Above the kinematic boundary, $\mathrm{Im}\,D^{-1}$ is nonzero. For $q>q^*$, it is

$$\mathrm{Im}\,D^{-1}=\frac{-\rho_0\pi\Omega}{2\alpha v_F q}. \tag{B7}$$

This leads to a pseudo-Lorentzian behavior for $\mathrm{Im}\,D$. The location of the maximum of $\mathrm{Im}\,D$, denoted as Γ, can be found upon differentiation with respect to Ω, leading to

$$\Gamma/E_x=0.5(q^*/k_F)^2(q/q^*)^3/\sqrt{\pi^2+\ln^2\frac{|q+q^*|}{|q-q^*|}}, \tag{B8}$$

which is also plotted in Fig. 8. If instead, we ignore the Ω term in Eq. (B5), we get Eq. (25) instead. The latter is a true Lorentzian, and its dispersion is plotted as well in Fig. 8. Although formally Eq. (B8) vanishes as q goes to q^*, the actual results based on Eq. (22a) do not, and we again find $c\sim 0.1$ in Eq. (26).

We finish this discussion by showing in Fig. 9 $\mathrm{Im}\,D$ based on Eq. (22a) for both positive and negative Ω for two cases, the quantum critical point ($\delta=0$) and somewhat away ($\delta=1$). The collective mode is not visible on the scale of this plot, but we note that it is only present on the positive frequency side. The damped response is approximately (anti)symmetric in Ω for $\delta=0$ but becomes highly asymmetric for nonzero δ. As δ increases, the most intense part of the damped response moves up the kinematic boundary $\Omega/E_x=1-q/q^*$ and approaches the logarithmic singularity at $q=0$ and $\Omega=E_x$. In Fig. 10, the dispersion of the $\mathrm{Im}\,D$ maxima is plotted for various δ. Note the reversed magnonlike dispersion of the undamped modes and the approximate linear q behavior of the damped modes for nonzero δ.

3. Free energy

Here we compute the free energy due to the excitations of the Kondo boson, whose expression is given by Eq. (27), and take into account all the different asymptotic structures of the propagator $D_\sigma(\mathbf{q},i\Omega_n)$ which are given in Eqs. (B1a)–(B1c), (B2a)–(B2d), and (B3a)–(B3e). The goal of this exercise is

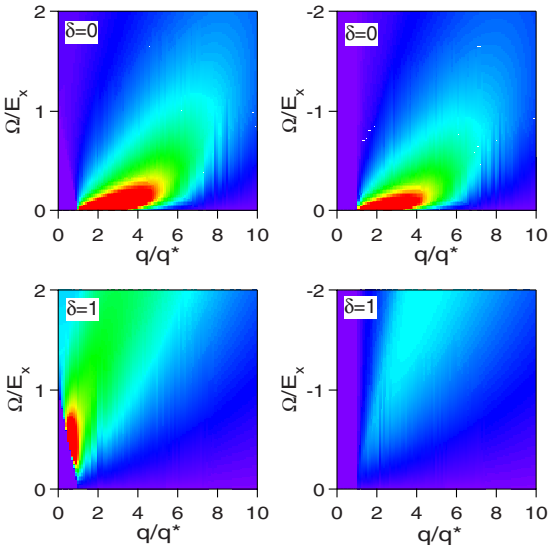

FIG. 9. (Color online) Plots of Im D for positive (left) and negative (right) Ω. The quantum critical point ($\delta=0$) is shown on the top, away from this ($\delta=1$) is shown on the bottom. The $z=2$ dispersion is not visible on the scale of this plot. Note the approximate (anti)symmetry of the damped ($z=3$) response at the QCP as compared to away. This damped dispersion at the QCP closely follows the analytic expression of Eq. (B8). The intensity scale for the bottom plots are a factor of 10 smaller than the top ones.

to prove that for all temperatures $T<\alpha D$, the leading contribution comes from that part of the phase space where the boson is overdamped with dynamical exponent $z=3$ and whose propagator is given by Eq. (25).

(1) $T<E^*$. Since for the leading T dependence we expect $\Omega\sim T$, in this temperature regime $D_\sigma(\mathbf{q},i\Omega_n)$ has three asymptotic forms which are given in Eq. (B1). Accordingly, we split the q integral into three parts, namely, $q<q_{\Omega 1}$, $q_{\Omega 1}<q<q^*$, and $q^*<q<k_F$, and denote their contributions as F_{1a}, F_{1b}, and F_{1c}, respectively. Keeping only the leading terms for each subregime, we get

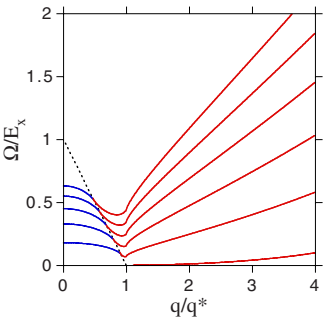

FIG. 10. (Color online) Dispersion of the Im D maxima for δ ranging from zero (bottom curve) to one (top curve). The undamped modes are to the left of the kinematic boundary (dashed line), while the damped modes to the right. Note the reversed magnonlike dispersion of the undamped modes and the approximate linear q behavior of the damped modes for nonzero δ.

$$F_{1a}=\frac{1}{4\pi^3}\int_{-\infty}^{\infty}d\Omega\,\coth\left(\frac{\Omega}{2T}\right)\int_0^{q_{\Omega 1}}dqq^2\,\mathrm{Im}\,\ln\left[-\frac{\Omega}{E_x}-i\eta\right]$$
$$=-\left(\frac{\pi^2}{90}k_F^3\right)\frac{T^4}{E_x^3},\tag{B9a}$$

$$F_{1b}=\frac{1}{4\pi^3}\int_{-\infty}^{\infty}d\Omega\,\coth\left(\frac{\Omega}{2T}\right)\int_{q_{\Omega 1}}^{q_*}dqq^2\,\mathrm{Im}\,\ln\left[\frac{q^2}{4k_F^2}-\frac{\Omega}{E_x}-i\eta\right]=-\left(\frac{\zeta(5/2)}{\pi^{3/2}}k_F^3\right)\frac{T^{5/2}}{E_x^{3/2}},\tag{B9b}$$

$$F_{1c}=\frac{1}{4\pi^3}\int_{-\infty}^{\infty}d\Omega\,\coth\left(\frac{\Omega}{2T}\right)\int_{q_*}^{k_F}dqq^2\,\mathrm{Im}\,\ln\left[\frac{q^2}{4k_F^2}-i\frac{\pi}{2}\frac{\Omega}{\alpha v_F q}\right]=-\left(\frac{k_F^3}{3}\right)\ln\left(\frac{k_F}{q^*}\right)\frac{T^2}{\alpha D}.\tag{B9c}$$

We note that, since $T<E^*$, the leading temperature dependence is due to the $z=3$ mode whose contribution is given by Eq. (B9c), and thus $F\approx F_{1c}$.

(2) $E^*<T<E_x$. In this temperature regime, $D_\sigma(\mathbf{q},i\Omega_n)$ has four asymptotic forms which are given in Eq. (B2). Now we split the q integral into four parts, namely, $q<q_{\Omega 2}$, $q_{\Omega 2}<q<q^*$, $q^*<q<q_{\Omega 3}$, and $q_{\Omega 3}<q<k_F$, and denote their contributions as F_{2a}, F_{2b}, F_{2c}, and F_{2d}, respectively. Once again, keeping only the leading terms for each subregime, we get

$$F_{2a}=\frac{1}{4\pi^3}\int_{-\infty}^{\infty}d\Omega\,\coth\left(\frac{\Omega}{2T}\right)\int_0^{q_{\Omega 2}}dqq^2\,\mathrm{Im}\,\ln\left[-\frac{\Omega}{E_x}-i\eta\right]$$
$$=-\left(\frac{\zeta(5/2)}{4\pi^{1/2}}k_F^3\right)\left(\frac{E^*}{\alpha D E_x^{3/2}}\right)T^{5/2},\tag{B10a}$$

$$F_{2b}=\frac{1}{4\pi^3}\int_{-\infty}^{\infty}d\Omega\,\coth\left(\frac{\Omega}{2T}\right)\int_{q_{\Omega 2}}^{q^*}dqq^2\,\mathrm{Im}\,\ln\left[-\frac{\Omega}{E_x}-i\eta\right]$$
$$=-\frac{(q^*)^3}{6\pi^2}T\ln\left(\frac{T}{E^*}\right),\tag{B10b}$$

$$F_{2c}=\frac{1}{4\pi^3}\int_{-\infty}^{\infty}d\Omega\,\coth\left(\frac{\Omega}{2T}\right)\int_{q_*}^{q_{\Omega 3}}dqq^2\,\mathrm{Im}\,\ln\left[-\left(\frac{q^*}{q}\right)\frac{\Omega}{\alpha v_F q}-i\frac{\pi}{2}\frac{\Omega}{\alpha v_F q}\right]=-\left(\frac{\Gamma(7/4)\zeta(7/4)}{6\pi^2}k_F^3\right)\left(\frac{q^*}{k_F}\right)^{3/4}\frac{T^{7/4}}{(\alpha D)^{3/4}},\tag{B10c}$$

$$F_{2d}=\frac{1}{4\pi^3}\int_{-\infty}^{\infty}d\Omega\,\coth\left(\frac{\Omega}{2T}\right)\int_{q_{\Omega 3}}^{k_F}dqq^2\,\mathrm{Im}\,\ln\left[\frac{q^2}{4k_F^2}-i\frac{\pi}{2}\frac{\Omega}{\alpha v_F q}\right]=-\left(\frac{k_F^3}{9}\right)\ln\left(\frac{\alpha D}{T}\right)\frac{T^2}{\alpha D}.\tag{B10d}$$

After comparing the various contributions above, once again we find that the leading temperature dependence is due to the

$z=3$ mode, whose contribution is given by Eq. (B10d), and we have $F \approx F_{2d}$.

(3) $E_x < T < \alpha D$. In this temperature regime $D_\sigma(\mathbf{q}, i\Omega_n)$ has five asymptotic forms which are given in Eq. (B3). Now we split the q integral into five parts, namely, $q < q_{\Omega 4}$, $q_{\Omega 4} < q < q^*$, $q^* < q < q_{\Omega 5}$, $q_{\Omega 5} < q < q_{\Omega 6}$, and $q_{\Omega 6} < q < k_F$, and denote their contributions as F_{3a}, F_{3b}, F_{3c}, F_{3d}, and F_{3e}, respectively. Once again, keeping only the leading terms for each subregime, we get

$$F_{3a} = \frac{1}{4\pi^3}\int_{-\infty}^{\infty} d\Omega \coth\left(\frac{\Omega}{2T}\right)\int_0^{q_{\Omega 4}} dq q^2 \,\mathrm{Im}\ln\left[\ln\left(-\frac{\Omega}{E_x} - i\eta\right) - \frac{E_x}{\Omega}\right] = -\left(\frac{(q^*)^3}{18\pi^2}\right)T, \tag{B11a}$$

$$F_{3b} = \frac{1}{4\pi^3}\int_{-\infty}^{\infty} d\Omega \coth\left(\frac{\Omega}{2T}\right)\int_{q_{\Omega 4}}^{q^*} dq q^2 \,\mathrm{Im}\ln\left[\ln\left(-\frac{\Omega}{E_x} - i\eta\right) + \frac{1}{6}\left(\frac{q}{q^*}\right)^2\right] = -\left(\frac{(q^*)^3}{12\pi^2}\right)T\ln\left(\frac{T}{E_x}\right), \tag{B11b}$$

$$F_{3c} = \frac{1}{4\pi^3}\int_{-\infty}^{\infty} d\Omega \coth\left(\frac{\Omega}{2T}\right)\int_{q^*}^{q_{\Omega 5}} dq q^2 \,\mathrm{Im}\ln\left[\ln\left(\frac{|\Omega|}{\alpha v_F q}\right) + 1 - i\frac{\pi}{2}\mathrm{sgn}(\Omega)\right] = -\left(\frac{\pi^2}{90}k_F^3\right)\frac{T^4}{(\alpha D)^3}, \tag{B11c}$$

$$F_{3d} = \frac{1}{4\pi^3}\int_{-\infty}^{\infty} d\Omega \coth\left(\frac{\Omega}{2T}\right)\int_{q_{\Omega 5}}^{q_{\Omega 6}} dq q^2 \,\mathrm{Im}\ln\left[\frac{\Omega^2}{2(\alpha v_F q)^2} - i\frac{\pi}{2}\frac{\Omega}{\alpha v_F q}\right] = -\left(\frac{\zeta(5/2)}{8\pi^{3/2}}k_F^3\right)\frac{T^{5/2}}{(\alpha D)^{3/2}}, \tag{B11d}$$

$$F_{3e} = \frac{1}{4\pi^3}\int_{-\infty}^{\infty} d\Omega \coth\left(\frac{\Omega}{2T}\right)\int_{q_{\Omega 6}}^{k_F} dq q^2 \,\mathrm{Im}\ln\left[\frac{q^2}{4k_F^2} - i\frac{\pi}{2}\frac{\Omega}{\alpha v_F q}\right] = -\left(\frac{k_F^3}{9}\right)\ln\left(\frac{\alpha D}{T}\right)\frac{T^2}{\alpha D}. \tag{B11e}$$

As before, we find that the leading temperature dependence is given by the $z=3$ mode, whose contribution is given by Eq. (B11e), and we have $F \approx F_{3e}$.

[1] G. Stewart, Rev. Mod. Phys. **73**, 797 (2001).
[2] H. von Lohneysen, A. Rosch, M. Vojta, and P. Wolfle, Rev. Mod. Phys. **79**, 1015 (2007).
[3] M. C. Aronson, R. Osborn, R. A. Robinson, J. W. Lynn, R. Chau, C. L. Seaman, and M. B. Maple, Phys. Rev. Lett. **75**, 725 (1995).
[4] A. Schroder, G. Aeppli, R. Coldea, M. Adams, O. Stockert, H. von Lohneysen, E. Bucher, R. Ramazashvili, and P. Coleman, Nature (London) **407**, 351 (2000).
[5] S. Araki, R. Settai, T. C. Kobayashi, H. Harima, and Y. Onuki, Phys. Rev. B **64**, 224417 (2001).
[6] J. A. Hertz, Phys. Rev. B **14**, 1165 (1976).
[7] A. J. Millis, Phys. Rev. B **48**, 7183 (1993).
[8] T. Moriya and T. Takimoto, J. Phys. Soc. Jpn. **64**, 960 (1995).
[9] A. Rosch, A. Schröder, O. Stockert, and H. v. Löhneysen, Phys. Rev. Lett. **79**, 159 (1997); A. Rosch, *ibid.* **82**, 4280 (1999).
[10] P. Coleman, C. Pepin, Q. Si, and R. Ramazashvili, J. Phys.: Condens. Matter **13**, R723 (2001).
[11] S. Pankov, S. Florens, A. Georges, G. Kotliar, and S. Sachdev, Phys. Rev. B **69**, 054426 (2004).
[12] Q. Si, S. Rabello, K. Ingersent, and J. L. Smith, Nature (London) **413**, 804 (2001); D. R. Grempel and Q. Si, Phys. Rev. Lett. **91**, 026401 (2003); P. Sun and G. Kotliar, *ibid.* **91**, 037209 (2003).
[13] P. Sun and G. Kotliar, Phys. Rev. Lett. **95**, 016402 (2005).
[14] L. De Leo, M. Civelli, and G. Kotliar, Phys. Rev. B **77**, 075107 (2008).
[15] T. Senthil, S. Sachdev, and M. Vojta, Phys. Rev. Lett. **90**, 216403 (2003); T. Senthil, M. Vojta, and S. Sachdev, Phys. Rev. B **69**, 035111 (2004).
[16] P. Coleman, J. B. Marston, and A. J. Schofield, Phys. Rev. B **72**, 245111 (2005).
[17] S. Paschen, T. Luhmann, S. Wirth, P. Gegenwart, O. Trovarelli, C. Geibel, F. Steglich, P. Coleman, and Q. Si, Nature (London) **432**, 881 (2004).
[18] J. Custers, P. Gegenwart, H. Wilhelm, K. Neumaier, Y. Tokiwa, O. Trovarelli, C. Geibel, F. Steglich, C. Pepin, and P. Coleman, Nature (London) **424**, 524 (2003).
[19] N. Read and D. M. Newns, J. Phys. C **16**, 3273 (1983); N. Read, *ibid.* **18**, 2651 (1985).
[20] A. J. Millis and P. A. Lee, Phys. Rev. B **35**, 3394 (1987).
[21] S. Burdin, D. R. Grempel, and A. Georges, Phys. Rev. B **66**, 045111 (2002); S. Burdin, M. Grilli, and D. R. Grempel, *ibid.* **67**, 121104(R) (2003).
[22] P. Fulde and R. A. Ferrell, Phys. Rev. **135**, A550 (1964); A. I. Larkin and Y. N. Ovchinnikov, Sov. Phys. JETP **20**, 762 (1965).
[23] T. M. Rice, Phys. Rev. B **2**, 3619 (1970).
[24] R. Hlubina and T. M. Rice, Phys. Rev. B **51**, 9253 (1995).
[25] I. Paul, C. Pepin, and M. R. Norman, Phys. Rev. Lett. **98**, 026402 (2007).
[26] C. Pepin, Phys. Rev. Lett. **98**, 206401 (2007); Phys. Rev. B **77**, 245129 (2008).
[27] Results for $d=2$ are discussed in Ref. 26.
[28] In gauge theories of strongly interacting systems, the standard large N expansion is known to break down due to the presence of infrared singularities. As shown in Ref. 26, the leading singularities can be controlled in an Eliashberg approach. Since our conclusions remain unchanged, in this paper, we ignore these technical complications.
[29] We assume a parabolic dispersion for the f spinons. As a consequence, the spinon susceptibility has a maximum at $q=0$, leading to a uniform solution for ϕ. In contrast, for a simple-cubic tight-binding lattice in $d=3$, the cosine dispersion of the f spinons gives rise to a logarithmic divergence of the spinon susceptibility at $\mathbf{q}=(\pi,\pi,\pi)$, resulting instead in a π flux phase solution for ϕ.
[30] I. Affleck and J. B. Marston, Phys. Rev. B **37**, 3774 (1988); J. B.

Marston and I. Affleck, *ibid.* **39**, 11538 (1989).
[31] L. B. Ioffe and A. I. Larkin, Phys. Rev. B **39**, 8988 (1989); N. Nagaosa and P. A. Lee, Phys. Rev. Lett. **64**, 2450 (1990); P. A. Lee and N. Nagaosa, Phys. Rev. B **46**, 5621 (1992); P. A. Lee, Phys. Rev. Lett. **63**, 680 (1989).
[32] Heavy fermion metals have complex Fermi surfaces where both conduction and f surfaces are large. As a consequence, large values of q^* are unlikely. Very small values of q^* are possible due to degeneracies. Within our simple model, a value of $q^*/k_F \sim 0.1$ is a reasonable estimate.
[33] S. Doniach, Physica B (Amsterdam) **91**, 213 (1977).
[34] T. Holstein, R. E. Norton, and P. Pincus, Phys. Rev. B **8**, 2649 (1973); M. Yu. Reizer, *ibid.* **40**, 11571 (1989); **44**, 5476 (1991).
[35] N. Nagaosa and P. A. Lee, Phys. Rev. B **61**, 9166 (2000); P. A. Lee, N. Nagaosa, and X.-G. Wen, Rev. Mod. Phys. **78**, 17 (2006).
[36] This marginal Fermi-liquid result is well known in related contexts; see, for instance, Refs. 2, 31, and 34.
[37] As we showed in Sec. IV B, Gaussian fluctuations about the mean-field solution generate a dispersion for the σ field. As a consequence of gauge invariance, this also implies a coupling between the σ and the gauge fields which leads to a back-flow current. From the point of view of an effective-field theory, where the σ fields are dressed, the constraint $J_{f,i}=0$ is generalized to $J_{f,i}+J_{\sigma,i}=0$ and leads to an additional contribution to the conductivity via the Ioffe-Larkin composition rules (Ref. 31). This contribution, though, is of order α and therefore does not change our findings, since $\alpha \ll 1$ (Ref. 26).
[38] J. M. Ziman, *Electrons and Phonons* (Oxford University Press, London, 1960), pp. 376–377.
[39] G. Knebel, R. Boursier, E. Hassinger, G. Lapertot, P. G. Niklowitz, A. Pourret, B. Salce, J. P. Sanchez, I. Sheikin, P. Bonville, H. Harima, and J. Flouquet, J. Phys. Soc. Jpn. **75**, 114709 (2006).
[40] Note that the $z=2$ modes make subleading contributions to all quantities but the crossover lines. They also make no contribution to the conduction-electron self-energy and transport due to kinematic constraints.
[41] For spherical Fermi surfaces, as many ordering wave vectors as allowed by lattice symmetry will condense, each with a modulus of q_0.
[42] See, e.g., A. L. Fetter and J. D. Walecka, *Quantum Theory of Many-Particle Systems* (Dover, New York, 2003), pp. 158–163.